

# We are IntechOpen, the world's leading publisher of Open Access books Built by scientists, for scientists

6,900

Open access books available

186,000

International authors and editors

200M

Downloads

Our authors are among the

154

Countries delivered to

TOP 1%

most cited scientists

12.2%

Contributors from top 500 universities



WEB OF SCIENCE™

Selection of our books indexed in the Book Citation Index  
in Web of Science™ Core Collection (BKCI)

Interested in publishing with us?  
Contact [book.department@intechopen.com](mailto:book.department@intechopen.com)

Numbers displayed above are based on latest data collected.  
For more information visit [www.intechopen.com](http://www.intechopen.com)



---

# Radial Ball Bearings with Angular Contact in Machine Tools

---

Ľubomír Šooš

Additional information is available at the end of the chapter

<http://dx.doi.org/10.5772/51004>

---

## 1. Introduction

The decisive criteria of the quality of machining tools are their productivity and working accuracy.

One innovated method for improving the technological parameters of manufacturing machines (machine tools) is to optimise the structure of their nodal points and machine components.

Because of the demands on machine tool productivity and accuracy, the spindle-housing system is the heart of the machine tool, Figure 1, [1]. Radial ball bearings with angular contact are employed in ever increasing arrays. The number of headstocks supported on ball bearings with angular contact is increasing proportionally with the increasing demands on the quality of the machine tool [2]. This is because these bearings can be arranged in various combinations to create bearing arrangements which can enable the reduction of both radial and axial loads. The possibility of varying the number of bearings, their preload value, dimensions and the contact angle of bearings used in the bearing nodes, creates a broad spectrum of combinations which enable us to achieve the adequate stiffness and high speed capabilities of the **Spindle-Bearings System (SBS)** [2], [3]. Adequate stiffness and revolving speed of the headstock are necessary conditions for meeting the manufacturing precision quality and machine tool productivity required by industry.

When designing a machine tool headstock, the starting point is the design of the spindle support, as this limits the stability, accuracy and production capacity of the machine by its stiffness and revolving speed. However, the parameters influencing the stiffness and frequency can *act in opposition to each other*. The selection of the type of bearing has to take into consideration the optimization of its stiffness and revolving speed characteristics. The maximum turning speed of the bearings is a function of the maximum revolving speed of

the individual bearings, their number, pre-load magnitude, manufacturing precision, and the types of lubrication used.

The stiffness of the SBS depends on the stiffness of the bearings and the spindle itself. There are several methods that can be employed for determining the static stiffness of the spindle system, e.g. [1] and [2].

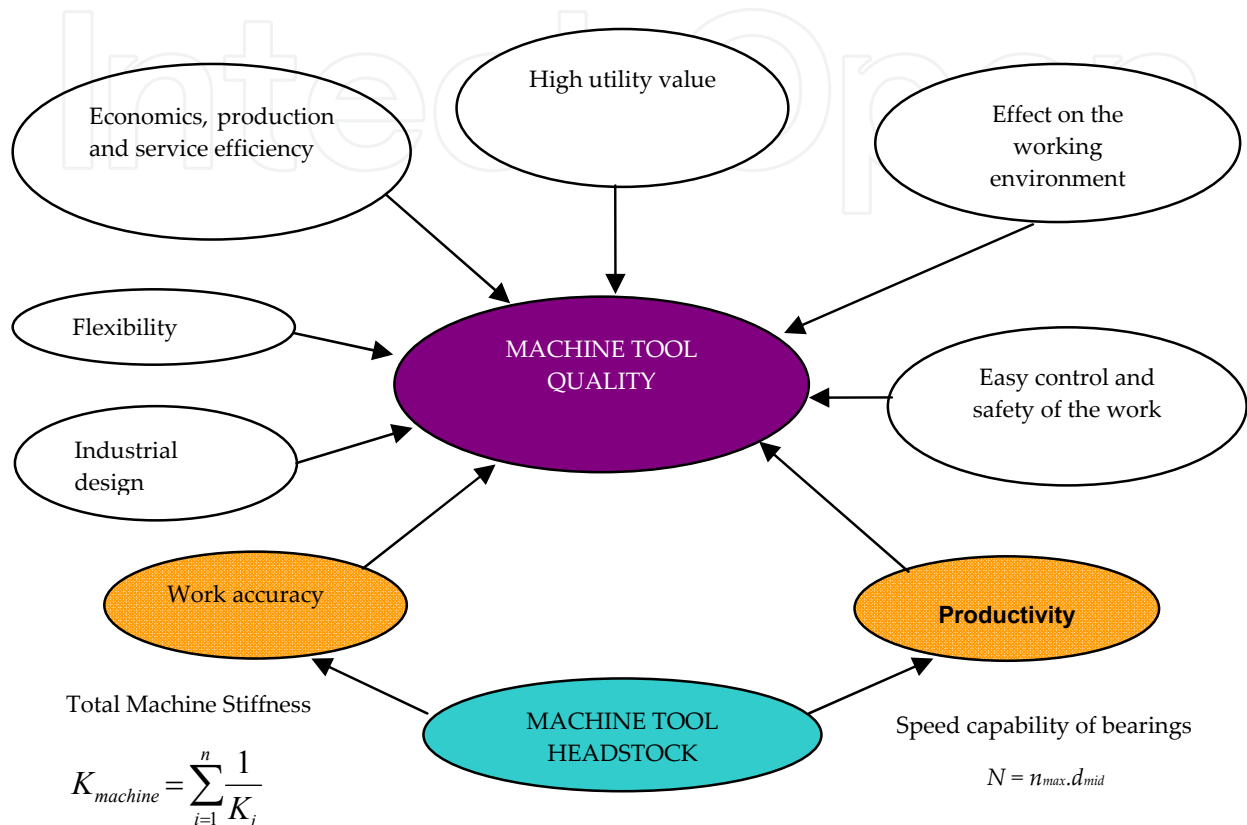


**Figure 1.** Factors influencing the Quality of Machine Tools, [4].

However, one problem which has not yet been solved is the calculation of the stiffness of the bearings, (or nodes of bearings) in the individual housing. Accurate calculation of the stiffness of the bearing nodes requires the determination of the static parameters of each bearing. From a mathematical point of view, this can be solved by using a system of non-linear differential equations, which requires the use of computers. To simplify the design, we need a static analysis which provides the basis for the dynamic characteristics of the mounting, and of the machine itself. Designers often prefer the conventional and proven methods of mounting, without taking into account the technical and technological parameters of the machine.

For the design engineer, it is important to be able to undertake a quick evaluation of various SBS variants at the preliminary design stage. The success of the design will depend on the correct choice of suitable criteria for the SBS, and if the design engineer has adequate experience in this field.

## 1.1. Headstock – The heart of the machine tool

The headstock, whether tool or workpiece carrier, has a direct influence on the static and dynamic properties of the cutting process, Figure 2. The spindle-bearing system (SBS) stiffness affects the surface quality, profile, and dimensional accuracy of the parts produced. It also has a direct influence on machine tool productivity because the width of cut influences the initiation of self-induced vibration; it is directly proportional to machine tool stiffness and damping.

Complex analysis of the SBS is very difficult and complicated, [5]. The analysis requires an advanced understanding of mathematics, mechanics, machine parts, elasto-hydrodynamic theory, rolling housing techniques, and also programming skills. The results of our research into SBS have been divided into three parts:

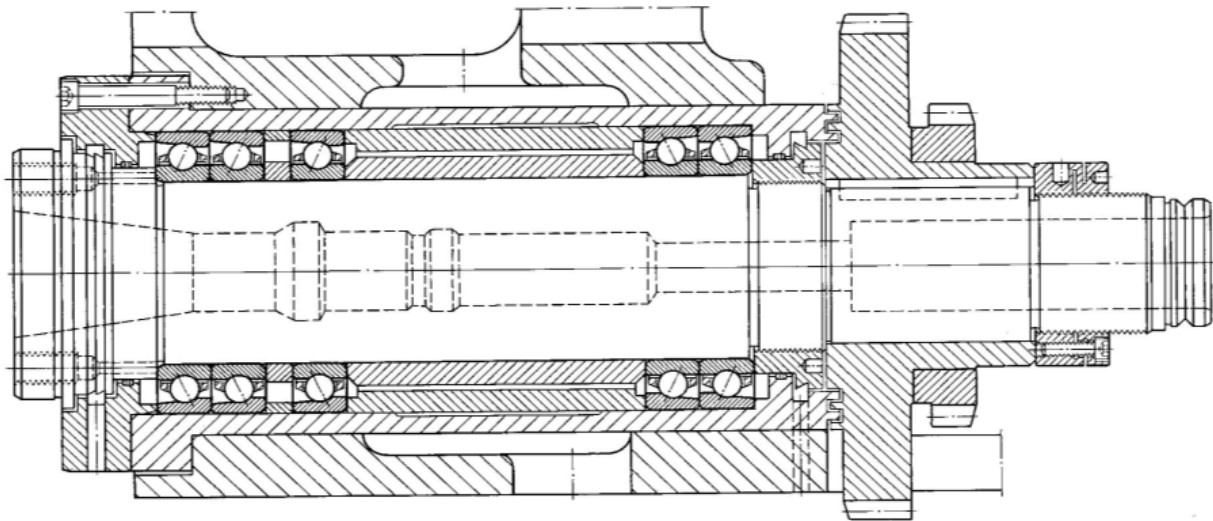


**Figure 2.** CNC profile milling machine, Carl Hurt Maschines, Germany; Work nodal point – 3x7013ACGA/P4, Opposite nodal point – 2x7013ACGA/P4

- Theoretical research - dealing with creating mathematical models
- Experimental research - verifying theoretical hypotheses and results on testing devices
- Application research - dealing with the special software application, *Spindle Bearings* for SBS design.

## 2. Theoretical research

A modular structure of the theoretical research is shown in Figure 3.

### 2.1. Primary static analysis

#### 2.1.1. Speed

The productivity of a machine tool, (Figure 1) can be increased in at least two different ways:

1. Externally - by shortening working time - within a working cycle
2. Internally - by reducing machining times (increasing the cutting width) - technological issues.

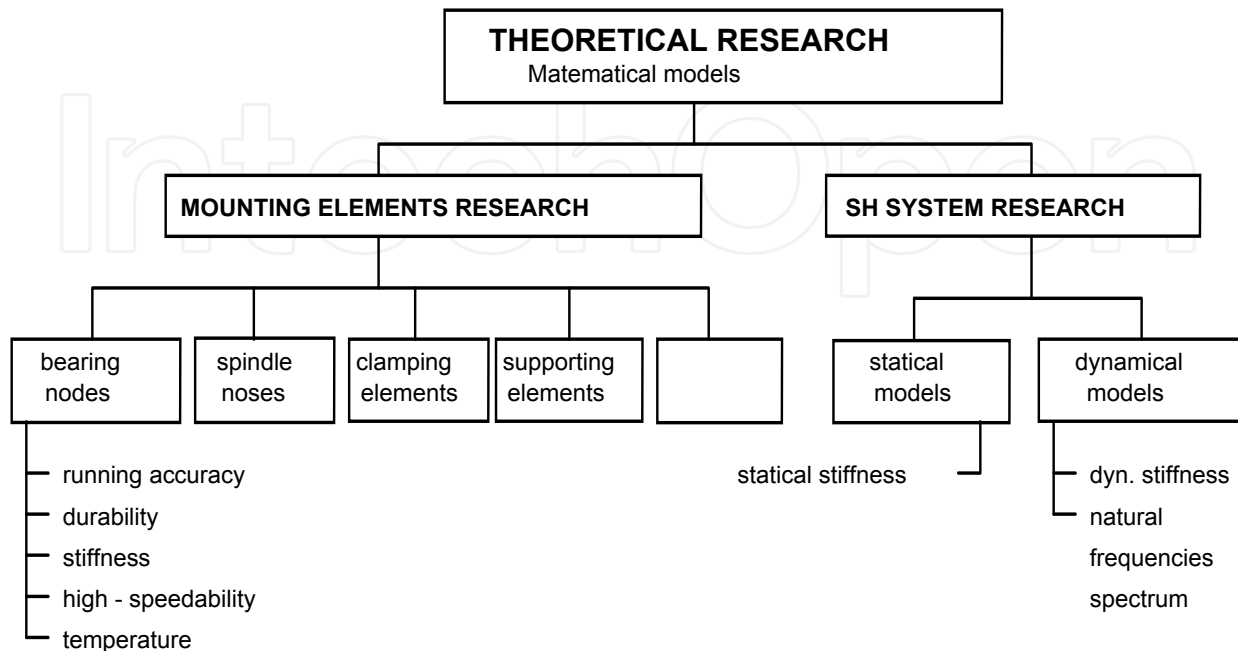


**Figure 3.** Modular structure of theoretical research, [5]

The philosophy of intelligent manufacturing systems applied to production processes minimise lost time. Further reducing lost time is expensive and has limited effectiveness at current levels of technological development. It has been shown that increased productivity can be achieved for example by changing the cutting speed. However this has a direct effect on tool life and on the dynamic stability of the cutting process.

The cutting speeds in machining processes depend on the technology applied, the cutting tool, and the workpiece material. The cutting speed also relates directly to the high-speed capability, and average diameter, of the bearings, the so-called factor  $N = n_{max} \cdot d_{mid}$ . Thus, from the point of view of the required cutting speed, the most important factor is the revolving frequency capacity of a spindle which is supported on a bearing system.

The calculation of the headstock's maximum revolving speed is relatively simple. The highest revolving speed of a bearing node is calculated on the basis of the highest revolving speed of one bearing, multiplied by various coefficients reflecting the influence on the bearings, the bearing arrangement, bearing precision, their preloaded value, and lubrication and cooling conditions.

### 2.1.2. Stiffness

The total static stiffness of machine tools is, in almost all cases, limited by the stiffness of the weakest parts. Amongst all the elements, the Spindle-Bearings System of the machine tool plays the most important role.

From results of structural analyses, the headstock can be considered as the heart of the whole machine tool. The design and quality of the machine tool must respect the quality of the drives and their features.

The headstock (as tool, or workpiece carrier), has a direct influence on the static and dynamic properties of the cutting process. The Spindle-Bearing System's stiffness also influences the final surface quality, profile, and dimensional accuracy of the workpiece.

The problem here is how quickly the headstock stiffness can be calculated with sufficient precision. The headstock stiffness must be calculated according to the deflection at the front end of the spindle, because the deflection at this point directly affects the precision of the finished product. The deflection at the spindle front end is the accumulation of various other, more or less important, partial distortions. The radial headstock stiffness can be calculated as follows:

$$K_{rc} = \frac{F_r}{y_{rc}} \quad (1)$$

The individual headstock parts, (spindle and bearing arrangement), create a serial spring arrangement and it is evident that the resulting stiffness  $K_{rc}$  is limited by the stiffness of the weakest part. An expert can see which part should be improved, and which partial distortions need to be minimized.

## 2.2. Simplified method of calculation

The calculation of spindle front end deflection, which takes into consideration all the important parameters, can only be achieved by using powerful computers. The analysis can be carried out by standard or custom software programs.

Calculating the many combinations of SBS arrangements is very demanding on time and money. Undertaking stiffness analysis using standard programs depends on the engineers' experience. The results can be open to questionable even when a suitable mathematical method is used (finite element method, boundary element method, Castilian's theorem, graphic Mohr's method, etc). This is because the headstock box, bearings or bearings nodes are statically indefinite systems which produce a nonlinear deformation of the node when under load.

Special software programmes are very expensive. They are developed using the most up-to-date theoretical and practical knowledge. These programs have been developed by research institutions and bearing producers and the possibility of using such programs significantly influences their position on the SBS market. Taking the above into account, engineers would benefit from the existence of a simplified method of static analysis. Such a methodology would enable the engineer at the preliminary design stage to limit the number of possible spindle-bearing variants and determine the direction which would lead to the optimal SBS design, [6].

The main methodological advantage of computer analysis is the possibility of repeating single calculating algorithms in a matrix shape. To this end a special software package, "Spindle Headstock" was developed at the Department of Production Engineering in the Faculty of Mechanical Engineering at STU, Bratislava, [7].

The resulting radial deformation,  $y_{rc}$ , of the front spindle end is shown in Figure 4.

Resulting static distortion of the front-end spindle equals

$$y_{rc} = y_0 + y_1 + y_t + y_a + y_v + y_{sb} + y_h \quad (2)$$

Our experience has shown that whatever mathematical method and software is used, the spindle distortion caused by *bending moments*  $y_0$  and by *bearing compliances*  $y_1$  have the greatest influence on the resulting front end spindle distortion, [6].

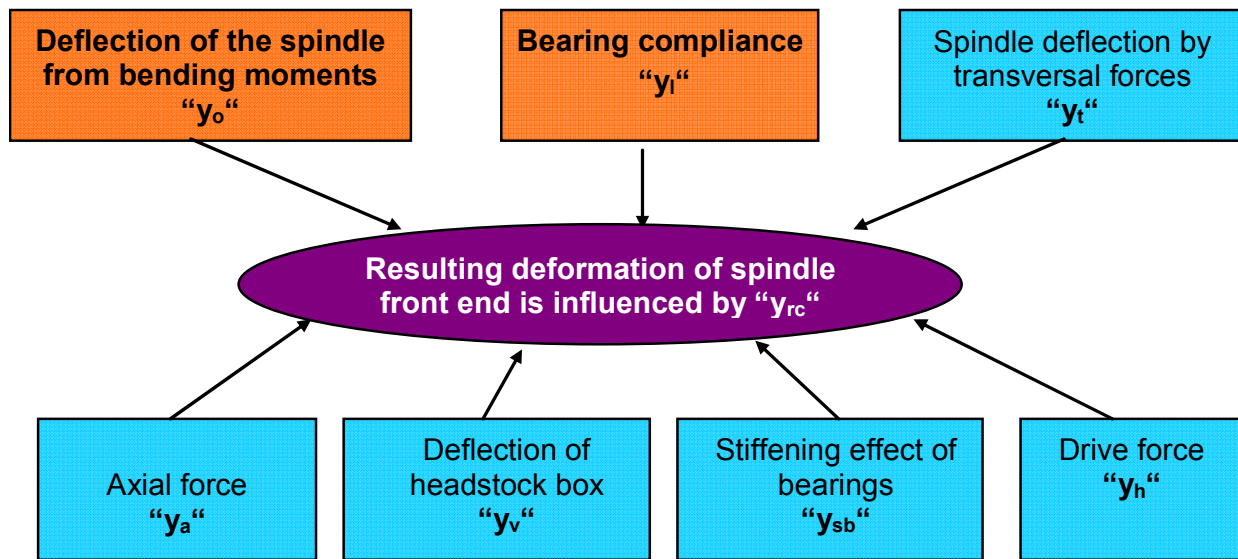


Figure 4. Factors influencing the resulting deflection

Then

$$y_{rc} = y_0 + y_1 \quad (3)$$

where the distortion caused by bending moments is as follows:

$$y_0 = \frac{F_r a^2}{3E} \left[ \frac{a}{J_a} + \frac{L}{J_L} \right] \quad (4)$$

and the deflection caused by bearing compliance is as follows:

$$y_1 = \frac{F_r}{L^2} \left[ \frac{a^2}{K_B} + \frac{(L+a)^2}{K_A} \right] \quad (5)$$

Increasing moments of inertia " $J_a$ ", " $J_L$ " were calculated as follows:

$$J_a = \frac{\pi}{64} [D_a^4 - d_a^4] \quad \text{and} \quad J_L = \frac{\pi}{64} [D_L^4 - d_L^4] \quad (6)$$

The definition of the quantities is shown in Figure 5. The individual headstock parts (spindle, bearing arrangement,) create a serial spring arrangement, and it is evident that the resulting stiffness  $K_{rc}$  is limited by the stiffness of the weakest part, [1] [2] and [9].

At the same time, parameters " $F_r$ ", " $a$ ", " $L$ " influence the value of both deflections. The spindle deflection caused by bending moments can be decreased by the following methods:

- increasing the material modulus of elasticity " $E$ ",
- increasing moments of inertia " $J_a$ ", " $J_L$ " by a change of spindle diameters " $D_a$ ", " $D_L$ ", " $d_a$ ", " $d_L$ ".

The resulting static distortion of the spindle front-end can be explicitly described by a multi-parametrical equation in the form of:

$$y_F = f [E, F_r, a, L, J_a, (D_a, d_a), J_L (D_L, d_L), K_A, K_B, \rho] \quad (7)$$

- spindle material and dimensions ( $E, D_a, d_a, D_L, d_L$ )
- loading forces position, orientation and magnitude ( $F_r, N, r_F, b$ )
- bearing arrangement configuration and stiffness ( $K_A, K_B$ )
- spindle and bearing arrangement space configuration ( $L, a$ )
- spindle box construction ( $k_{\xi}, \rho$ )

There remains one significant problem with the calculation of the bearing nodes, and that is that they are statically indeterminate systems.

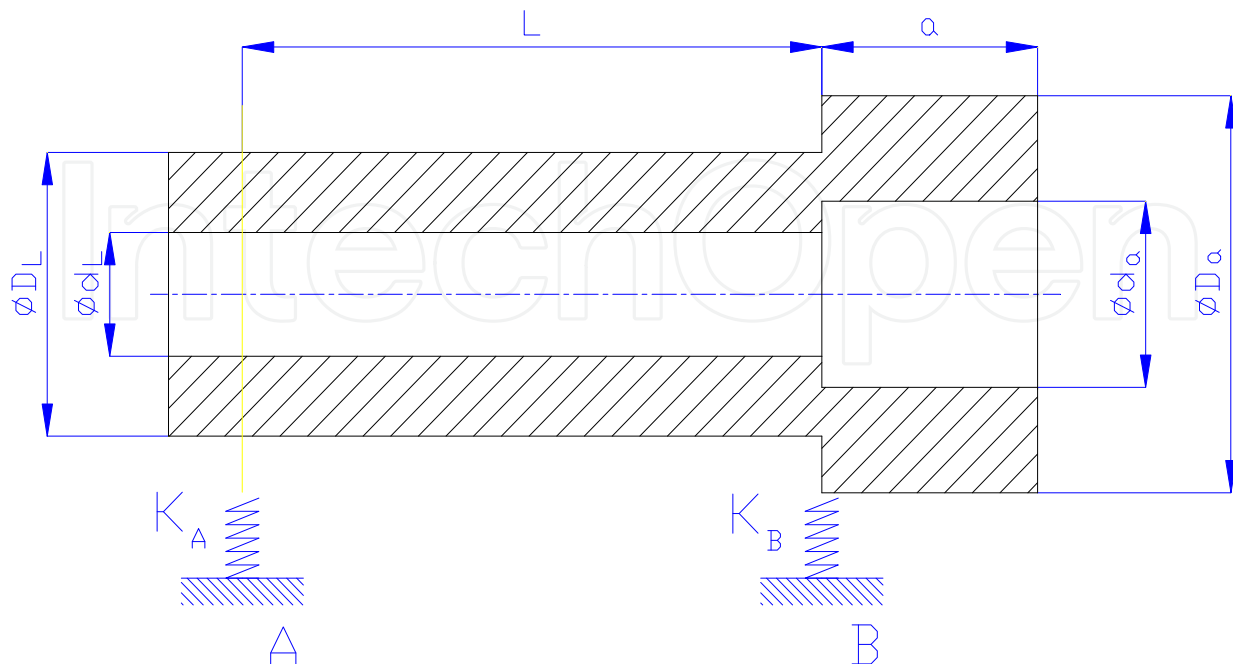


**Figure 5.** Cross section scheme of the spindle-bearing system

### 2.3. Dynamic analysis

While static analysis of *SBS* describes spindle behaviour in a static mode, dynamic analysis describes *SBS* behaviour under real conditions, in real running time, and so the real operational state is better represented. It is very important to know the dynamic characteristics, especially in high-speed headstocks. It is important to ensure that the operational revolving frequencies do not fall within the resonant zone. When this happens, the vibration amplitude of the spindle is considerably increased, and the spindle's total stiffness falls to unacceptable levels.

The most common determining dynamic characteristics of *SBS* are:

- the spectrum of natural (resonant) frequencies (usually the first three frequencies),
- the amplitudes of vibrations along the spindle independent of the revolving frequencies of the spindle,
- the resonant amplitudes of vibrations,
- the dynamic stiffness of the spindle (at the given speed of the spindle).

The *SBS* dynamic properties (dynamic deflection of spindle front-end, natural frequencies spectrum) [5], are affected by factors shown in Figure 6.

#### Mathematical models for determining the dynamic properties of a spindle

Currently, the only reliable method for determining dynamic properties is to use experimental measurements. Therefore it is very useful to create reliable mathematical models for determining these dynamic properties.

In line with spindle mass reduction, mathematical models are divided into:

- 1/ discrete with 1<sup>o</sup>, 2<sup>o</sup> and N<sup>o</sup> degrees of freedom,
- 2/ continuous.

The discrete mathematical model developed for measuring the revolving vibration of spindles with N<sup>o</sup> degrees of freedom is worked out in [1], [5]. This mathematical model for calculating the dynamic properties of the spindle enables us to include in our calculation the effects of the materials, the dimensions of the rotating parts, the bearing node stiffness, and the radial forces generated by the cutting process and drive. The results calculated reflect a spectrum of natural frequencies and the dynamic deflection of the spindle under discrete masses.

The deflection of spindle  $y_i$  loaded with concentrated forces at the  $i^{\text{th}}$  point can be expressed in the form:

$$y_i = a_{i1}F_{1o} + a_{i2}F_{2o} + \dots + a_{ik}F_{ko} + \dots + a_{in}F_{no} \quad (\text{m}) \quad (8)$$

where  $a_{jk}$  (m/N) is Maxwell's affecting factor. Every mass point on the spindle produces centrifugal force

$$F_{io} = m_i y_i \omega^2 \quad (\text{N}) \quad (9)$$

where  $m_i$  (kg) is mass  $i^{\text{th}}$  discrete segment.

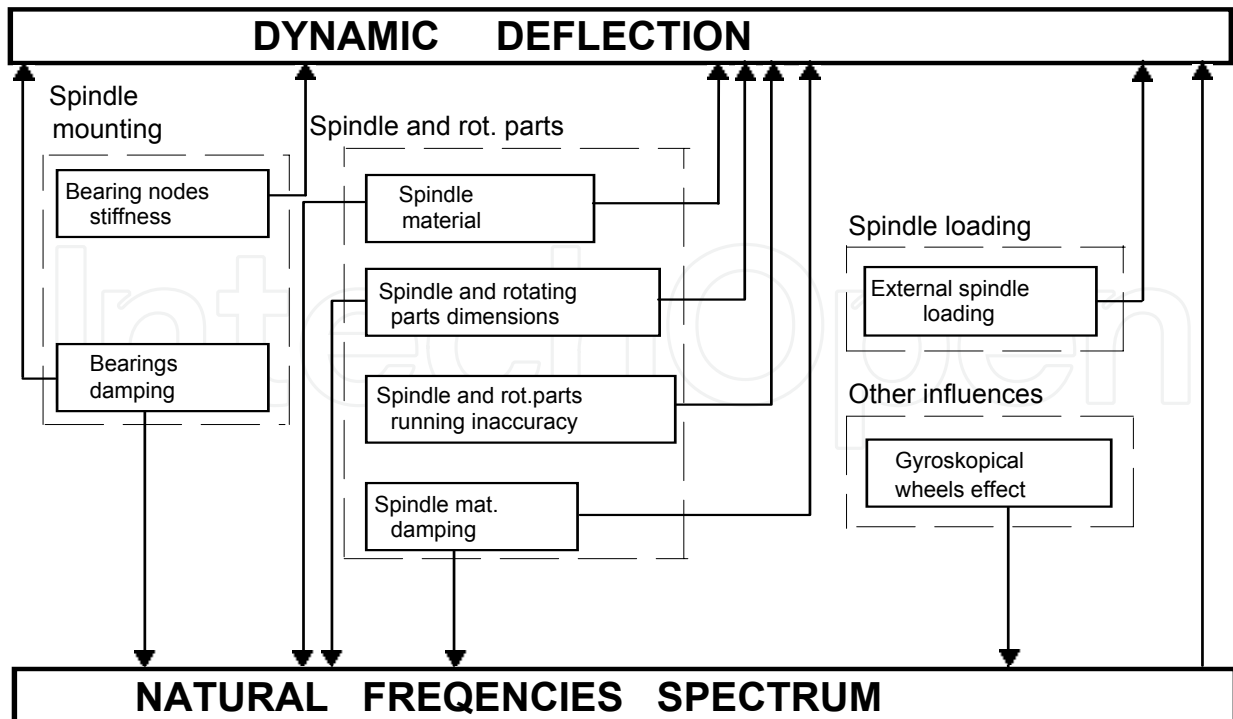


**Figure 6.** Factors affected by SBS dynamic properties

The application of the aforementioned equations and their modification for masses of “n” value, will create a system of homogenised algebraic equations where the results of determinant D are angular natural frequencies of the transverse vibrations of the spindle  $\omega_i$  ( $\text{rad.s}^{-1}$ ).

The procedure for determining the dynamic deflections  $y_i$ , when the dimensions of the spindle, rotating parts, stiffness of bearing arrangement, and the external radial forces are taken into consideration, is very similar to the previous one. These procedures are described in [6].

$$\Delta = \begin{vmatrix} 1 - a_{11} m_1 \omega^2 & -a_{12} m_2 \omega^2 & \dots & -a_{1n} m_n \omega^2 \\ -a_{21} m_1 \omega^2 & 1 - a_{22} m_2 \omega^2 & \dots & -a_{2n} m_n \omega^2 \\ \dots & \dots & \dots & \dots \\ -a_{n1} m_1 \omega^2 & -a_{n2} m_2 \omega^2 & \dots & 1 - a_{nn} m_n \omega^2 \end{vmatrix} = 0 \quad (10)$$

It is relatively easy to transform this mathematical model into a computer readable format and the calculation of the dynamic characteristics can be quickly achieved.

## 2.4. Theoretical research on bearing nodes

### 2.4.1. Arrangements of nodal points

Usually, radial ball bearings with angular contact arrangements in their nodal points contain 2, 3 or more bearings, see Figure 7.

### 2.4.2. Criteria for selecting the arrangement of bearings

The number of spindle bearing systems supported on ball bearings with angular contact increases proportionally with increasing demand on the machine tool. By varying the bearings and their arrangement in the bearing nodes (DB, DF, DT, TBT, TTF, QBC, ..), the value of the contact angle, magnitude of preload, and type of flanges can be optimized to suit the required, resulting stiffness and speed-capability of the spindle-bearing system.

In order to assess the maximum permissible speed of different types of spindle rotations, a parameter for the so-called high-speed characteristics has been introduced:  $N = n_{max} \cdot d_{mid}$ , where " $n_{max}$ " denotes the maximum spindle revolutions and " $d_{mid}$ " the medial diameter of the bearings. Following this parameter, roller bearings of machine tool spindles can be divided into 3 basic groups, [10]:

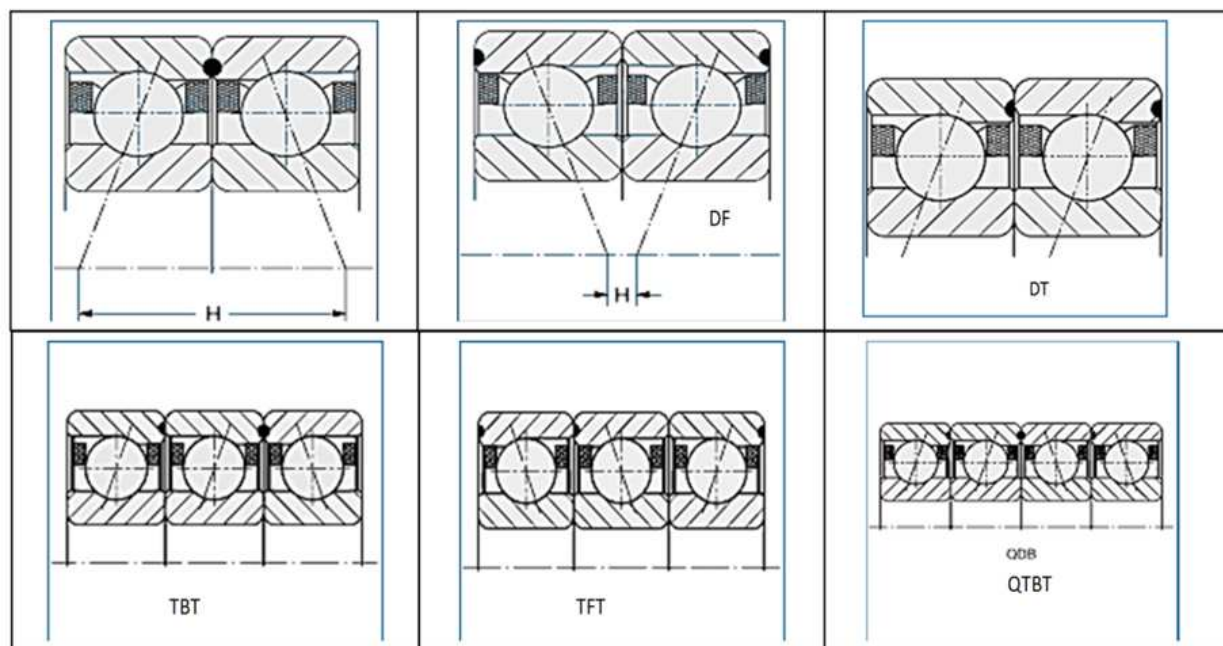


**Figure 7.** Arrangements in nodal points

GROUP 1:  $N = (0,1 - 0,5) \cdot 10^6$ : Headstocks of heavy duty machines for turning, milling and drilling operations. In these machines the spindles are predominantly mounted using double-row roller bearings in combination with axial ball bearings, or tapered bearings. We can assume that the linearization of the deformation curve in roller bearings is sufficiently accurate, which simplifies the calculation of the radial stiffness of the nodal point, [2]. These *mountings* offer high stiffness and load-bearing capacity and quiet operation.

GROUP 2:  $N = (0,4 - 1) \cdot 10^6$  is characterized by bearings of medium size and are found in smaller NC and CNC turning, milling, drilling and grinding machine tools. The maximum possible speed in bearings with linear joints is limited by the heat produced in the head, and

therefore they are used only for the mounting of spindles with the lowest values of coefficient  $N$ . Developments in the field of increased speed capability is focused on bearings with point contacts, as these have better friction characteristics.

GROUP 3: Spindles mounted in bevelled radial bearings with optimized structure (design) and using new composite materials enabling high-speed operation,  $N = (0.8 - 2.5) \times 10^6$  which is typical for high-speed machining.

Spindle mountings using only radial bevelled bearings, (table 1), [11] can be divided into 2 basic types:

- spindles mounted on bearing nodes with “directionally” arranged bearings, with equal orientation of contact angles in each nodal point 1, 2, 3, and 7, table 1.
- spindles mounted on nodal points with bearings arranged according to shape. Bearings are arranged in “O” or (X) shape, in combination with “T”.

A typical feature of the nodes of spindle bearings is the application of pre-stressing, which provides the stiffness of the nodal point and reduces any skidding of the rollers at high revolutions.

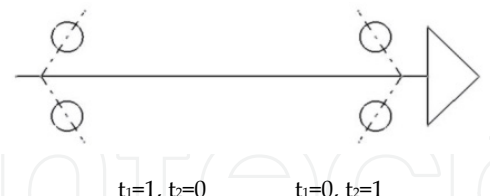
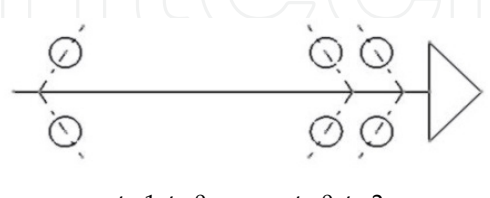
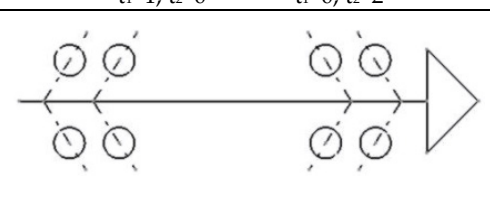
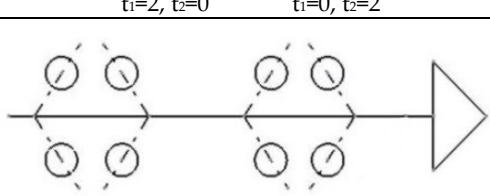
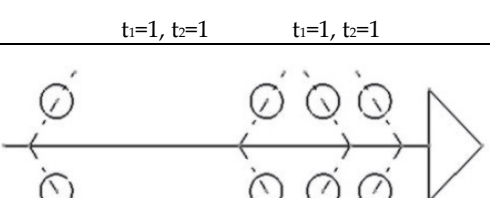
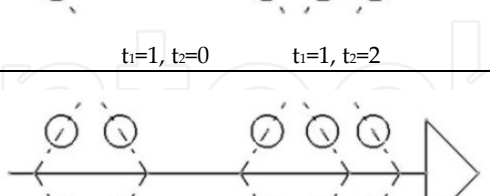
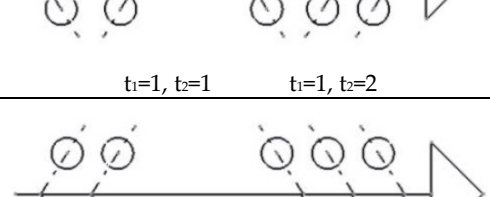
Pre-stressing can be achieved through three flange design principles:

- a. Sprung flange: thermal expansion (dilatation) is eliminated by changing the length of the elastic materials positioned between the flange and the bearings, which ensures minimum change in the pre-stress value.
- b. Stiff (Rigid) flange: provided by a fixing nut or casing. This design provides better stiffness characteristics. The pre-stress value is changed due to the influence of thermal dilatation.
- c. Controllable flange: axially adjustable (by means of hydraulics), which ensures the required pre-stressing for different operational conditions.

The highest values of the coefficient  $N$  can be achieved by using spindles mounted on nodes with a “directional” arrangement of bearings, 1, 2 and 3. When used in conjunction with the controllable flange, the correct types of lubrication and cooling, speeds which are comparable with the maximum revolutions of the bearings themselves can be achieved. Thus they can be applied in high-speed machining [11]. These mounting types, in combination with the sprung support, are mostly used for grinding.

For difficult technological operations requiring considerably higher stiffness in the radial and axial directions, nodal points with bearings arranged according to shape, together with fixed supports are typical.

There is negligible use of hybrids of the basic types of mounting (mounting 5), as shown in table 1. In such cases one nodal point has bearings arranged according to shape, while the other has directionally arranged bearings, (Figure 2). The pre-stressing in the front nodal point is ensured by a stiff flange, and in the rear nodal point by a sprung flange.

Seq. No.	CONFIGURATION		$N = n_{max} \cdot d_{mid} \cdot 10^6$ [mm.min <sup>-1</sup> ]	Characteristic	Use
	Rear bearing node	Forward bearing node			
1.	 <p><math>t_1=1, z_1=0</math>      <math>t_1=0, z_1=1</math></p>	1,2 - 2,5	<ul style="list-style-type: none"> <li>- single direction of rotation</li> <li>- light axial and radial loads</li> </ul>	- grinding internal holes	
2.	 <p><math>t_1=1, z_1=0</math>      <math>t_1=0, z_1=2</math></p>	0,8 - 1,6	<ul style="list-style-type: none"> <li>- suitable for extremely short spindles</li> <li>- medium axial loads</li> </ul>	<ul style="list-style-type: none"> <li>- finishing machines</li> <li>- drilling of deep holes</li> </ul>	
3.	 <p><math>t_1=2, z_1=0</math>      <math>t_1=0, z_1=2</math></p>	0,8 - 1,4	<ul style="list-style-type: none"> <li>- medium radial loads</li> <li>- very common method of use</li> </ul>	<ul style="list-style-type: none"> <li>- grinding internal holes</li> <li>- milling</li> <li>- drilling</li> </ul>	
4.	 <p><math>t_1=1, z_1=1</math>      <math>t_1=1, z_1=1</math></p>	0,6 - 1	<ul style="list-style-type: none"> <li>- machining light metals</li> <li>- medium radial loads</li> </ul>	<ul style="list-style-type: none"> <li>- grinding</li> <li>- precision drilling</li> <li>- turning/ lathe</li> </ul>	
5.	 <p><math>t_1=1, z_1=0</math>      <math>t_1=1, z_1=2</math></p>	0,5 - 0,9	<ul style="list-style-type: none"> <li>- medium axial loads</li> </ul>	<ul style="list-style-type: none"> <li>- drilling of deep holes</li> <li>- milling</li> </ul>	
6.	 <p><math>t_1=1, z_1=1</math>      <math>t_1=1, z_1=2</math></p>	0,4 - 0,9	<ul style="list-style-type: none"> <li>- medium axial loads</li> <li>- very common method of use</li> </ul>	<ul style="list-style-type: none"> <li>- turning/ lathe</li> <li>- drilling</li> </ul>	
7.	 <p><math>t_1=2, z_1=0</math>      <math>t_1=3, z_1=0</math></p>	0,3 - 0,6	<ul style="list-style-type: none"> <li>- high axial loads</li> <li>- medium radial loads</li> </ul>	<ul style="list-style-type: none"> <li>- milling</li> <li>- boring</li> </ul>	

**Table 1.** Type of SBS using radial ball bearings with angular contact [11]

### 2.4.3. Stiffness

The stiffness of the bearing arrangement ( $K_A, K_B$ ) is the specific parameter which influences the consequent spindle distortion. We have developed a simplified mathematical model for calculating radial and axial stiffness, [11], [12].

## 3. The calculation of radial stiffness of nodal points

### 3.1. Assumptions of solution

According to the Hertz assumptions [13], [14], there is a dependence between load "P" and deformation "δ" at the contact point of the ball with the plane, given by the relationship

$$P = k_{\delta} \cdot \delta^{3/2} \quad (11)$$

- the bearings in the nodal points are of the same type and dimensions, with precise geometric dimensions
- the value of the contact angle is the same for all directionally-arranged bearings in the nodal point, which delivers equal distribution of strain on these bearings
- radial load is equally distributed onto all the bearings in the nodal point

### 3.2. Stiffness of nodal points with directionally-arranged bearings

The calculation of the stiffness of a nodal point is based on the stiffness of the bearing itself [15], which is defined as:

$$K_{r1} = \frac{d F_{r1}}{d \delta_{r0}} \quad (12)$$

As radial displacement  $\delta_{r0}$  is a function of contact deformation  $\delta_0$  of the ball with the highest load [13], the equation for calculating the stiffness of bevelled radial bearings will have the form:

$$K_{r1} = \frac{d F_{r1}}{d \delta_0} \cdot \frac{d \delta_0}{d \delta_{r0}} \quad (13)$$

When calculating stiffness, the distribution of load among the rollers must be determined, and the dependence between the load on the top ball and external load must be found. The distribution of load in the bearing can be derived from the balance under static conditions [14],

$$F_{r1} = \frac{F_{r1}}{i} = \sum_{j=0}^z P_j \cdot \cos(\alpha_j) \cdot \cos(j \cdot \gamma) \quad (14)$$

where  $\gamma = \frac{360}{z}$  is the spacing angle of the balls.

The values of contact deformations  $\delta_j$  and angles  $\alpha_j$  differ from each other around the circumference of the bearing and can be expressed as follows, (Figure 8).

$$\delta_j = l_{rj} - l_p = \sqrt{\left[l_z \cdot \sin(\alpha_z) + \delta_p\right]^2 + \left[l_z \cdot \cos(\alpha_z) + \delta_{r0} \cdot \cos(j \cdot \gamma)\right]^2} - l_p \quad (15)$$

$$\cos(\alpha_j) = \frac{l_z \cdot \cos(\alpha_z) + \delta_{r0} \cdot \cos(j \cdot \gamma)}{\sqrt{\left[l_z \cdot \sin(\alpha_z) + \delta_p\right]^2 + \left[l_z \cdot \cos(\alpha_z) + \delta_{r0} \cdot \cos(j \cdot \gamma)\right]^2}} \quad (16)$$

By loading the pre-stressed bearing with a radial force, the distance,  $O_A O_{ip}$ , between the centre of the balls is constant, (Figure 8 b, c).

$$l_p \cdot \sin(\alpha_p) = l_{rj} \cdot \sin(\alpha_{rj}) = konst. \quad (17)$$

The dependence between the deformation of the  $j^{\text{th}}$  ball and the top ball can be determined by the relation

$$\delta_j = \delta_0 \cdot \cos(j \cdot \gamma) \quad (18)$$

By derivation of equation (14) we get

$$\frac{d F_{r1}}{d \delta_0} = i \cdot \sum_{j=0}^z \left[ \frac{d P_j}{d \delta_j} \cdot \cos(\alpha_j) - P_j \cdot \sin(\alpha_j) \cdot \frac{d \alpha_j}{d \delta_j} \right] \cdot \frac{d \alpha_j}{d \delta_0} \cdot \cos(j \cdot \gamma) \quad (19)$$

The unknown derivatives in equation (19) can be calculated by changing the relations (11), (17), (18).

$$\frac{d P_j}{d \delta_j} = \frac{3}{2} k_\delta^{2/3} P_j^{1/3} \quad (20)$$

$$\frac{d \alpha_j}{d \delta_j} = -\frac{\operatorname{tg}(\alpha_j)}{l_{rj}} \quad (21)$$

$$\frac{d \delta_j}{d \delta_0} = \cos(j \cdot \gamma) \quad (22)$$

The interdependence of the contact deformation and radial displacement, Figure 8, can be determined from the relation

$$\frac{d \delta_0}{d \delta_{r0}} = \left( \frac{d \delta_j}{d \delta_0} \right)^{-1} \cdot \frac{d \delta_j}{d \delta_{r0}} \quad (23)$$

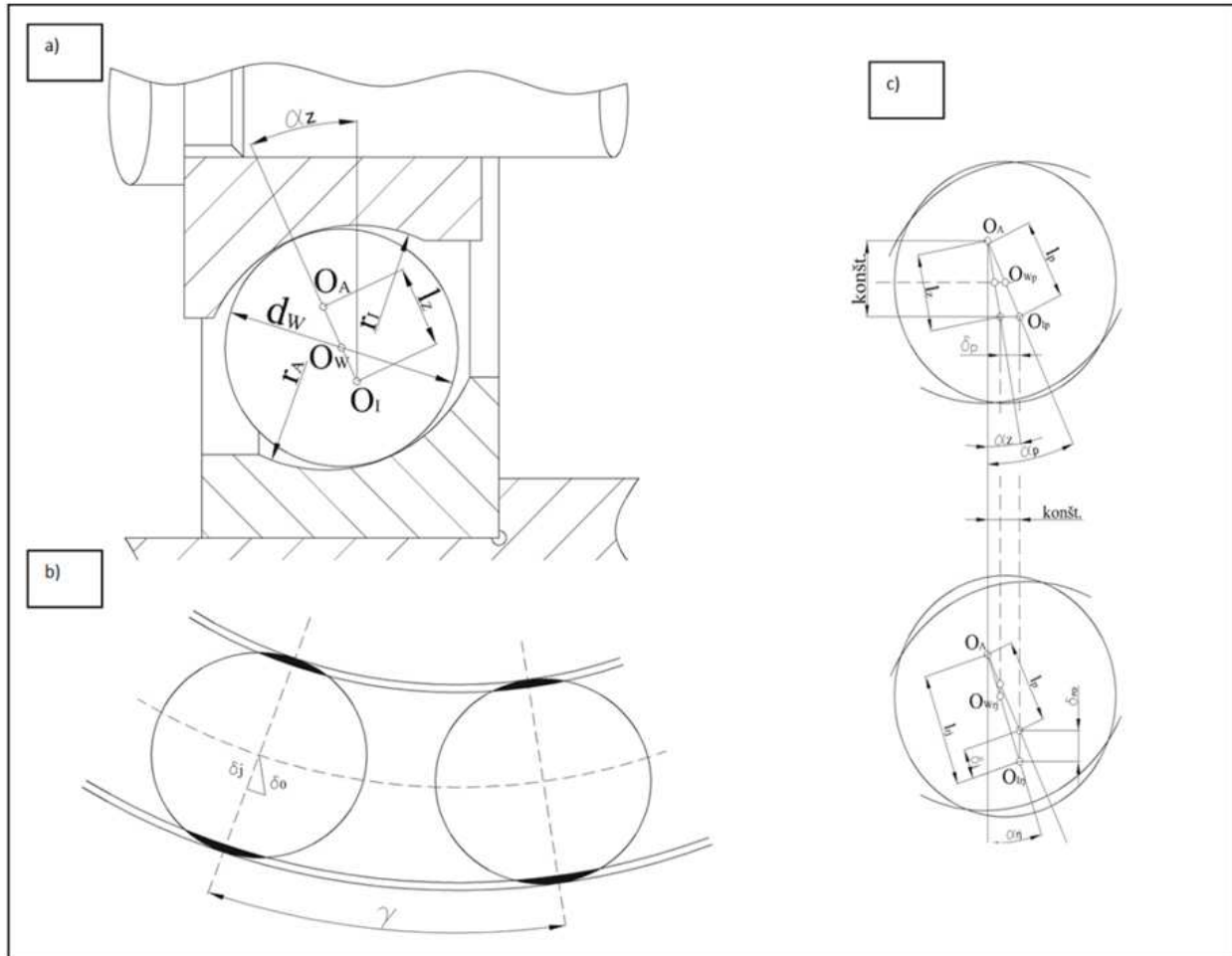


**Figure 8.** Detailed bearing scheme, a – unloaded, b – pre-stressed, c – radial loaded

Where  $\frac{d \delta_j}{d \delta_{r0}}$  is calculated from equation (15)

$$\frac{d \delta_j}{d \delta_{r0}} = \frac{1}{2} \cdot \frac{2(1_z \cos \alpha_z + \delta_{r0} \cos(j \cdot \gamma)) \cos(j \cdot \gamma)}{\sqrt{(1_z \cos \alpha_z + \delta_{r0} \cos(j \cdot \gamma))^2 + (1_z \sin \alpha_z + \delta_p)^2}} = \cos \alpha_j \cos(j \cdot \gamma) \quad (24)$$

by inserting equations (24) and (22) into equation (23)

$$\frac{d \delta_0}{d \delta_{r0}} = \frac{1}{\cos(j \cdot \gamma)} \cdot \cos(\alpha_j) \cdot \cos(j \cdot \gamma) = \cos(\alpha_j) \quad (25)$$

After inserting equations (25) and (19) into equation (13) we get the resulting relation for the stiffness of a pre-stressed nodal point with directionally-arranged bearings.

$$K_r = i \cdot \sum_{j=0}^z \left[ \frac{3}{2} \cdot k_s^{2/3} \cdot P_j^{1/3} \cdot \cos^2(\alpha_j) + P_j \cdot \frac{\sin^2(\alpha_j)}{l_{rj}} \right] \cdot \cos^2(j \cdot \gamma) \quad (26)$$

### 3.3. Stiffness of nodal point with bearings arranged according to shape

When calculating the nodal point with bearings arranged according to shape, we divide the nodal point into part "1" and part "2" (Table 1), with the *same* orientation of contact angles in nodes with directionally-arranged bearings, and the stiffness of the parts is calculated as follows:

$$K_{r1} = i_1 \cdot \sum_{j=0}^z \left[ \frac{3}{2} \cdot k_{\delta}^{2/3} \cdot P_j^{1/3} \cdot \cos^2(\alpha_{1j}) + P_j \cdot \frac{\sin^2(\alpha_{1j})}{l_{r1j}} \right] \cdot \cos^2(j \cdot \gamma) \quad (a)$$

$$K_{r2} = i_2 \cdot \sum_{j=0}^z \left[ \frac{3}{2} \cdot k_{\delta}^{2/3} \cdot P_j^{1/3} \cdot \cos^2(\alpha_{2j}) + P_j \cdot \frac{\sin^2(\alpha_{2j})}{l_{r2j}} \right] \cdot \cos^2(j \cdot \gamma) \quad (b)$$
(27)

For example in Figure 9 the total numbers of bearings in the front node SBS is 5:  $i_1 = 3$ ,  $i_2 = 2$ , contact angles  $\alpha_1 = \alpha_2 = 25$ .

We determine the total stiffness of the nodal point by the addition of both parts of the node with the equation:

$$K_r = K_{r1} + K_{r2} \quad (28)$$

In order to optimize the stiffness and load-bearing capacity for specified technological conditions, the manufacturers of machine tools have come out with a new, non-traditional solution for nodal points. By diminishing the contact angle of the bearing in Part 2, the axial stiffness of the nodal point is partially decreased, but at the same time, the value of the radial stiffness and boundary axial load is increased.

### 3.4. Approximate calculation of stiffness

When evaluating the overall stiffness of a spindle, the designer must take into account the approximate calculation of the stiffness of the nodal points.

If all the balls are loaded, and there are more than 2 per bearing [14], the following equation can be applied:

$$\sum_{j=0}^z \cos^2(j \cdot \gamma) = \frac{z}{2} \quad (29)$$

If the bearing angle is loaded only in an axial direction by the pre-stressing force, then the load on the rollers is constant around the whole circumference and can be expressed, for the particular parts of the nodal point [11] in the form

$$P_{1j} = \frac{F_p}{i_1 \cdot z \cdot \sin(\alpha_{p1})}; \quad P_{2j} = \frac{F_p}{i_2 \cdot z \cdot \sin(\alpha_{p2})} \quad (30)$$

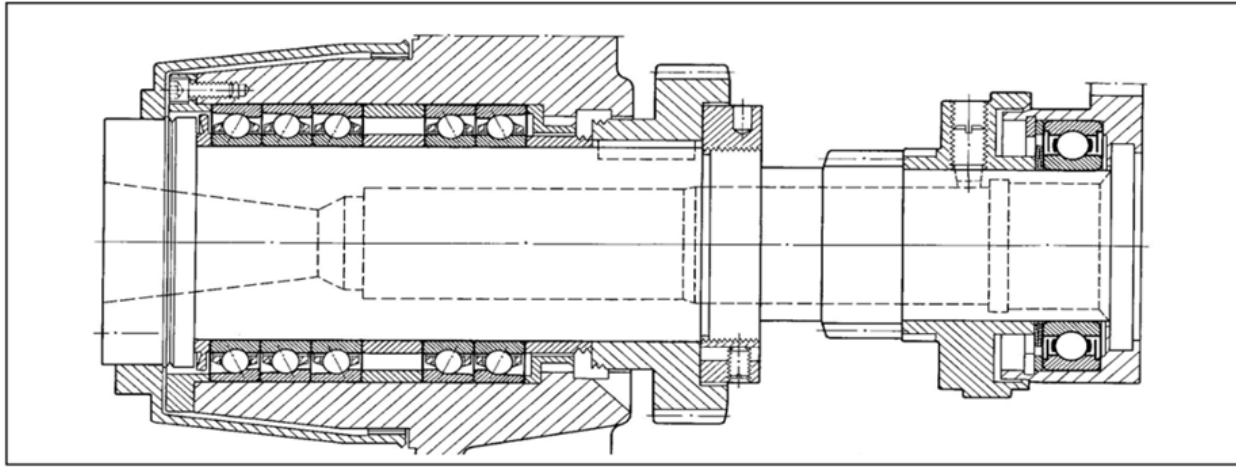


**Figure 9.** Horizontal machining centre, Thyssen-Hüller Hille GmbH, Germany; Work nodal – 3x71914 ACGB/P4 - 2x71914 ACGB/P4, Opposite side– 6011-2Z

If the magnitude of the spindle bearing contact angles is not greater than 26 degrees, then the value of the second expression in equations (27a) and (27b) is negligible.

Taking these assumptions into consideration, we obtain the relationship for the approximate calculation of the radial stiffness of a bearing angle with directionally placed bearings in the form:

$$K_r = \frac{3 \cdot 10^{-3}}{4} \cdot z^{2/3} \cdot k_\delta^{2/3} \cdot i_1^{2/3} \cdot F_p^{1/3} \cdot \frac{\cos^2(\alpha)}{\sin^{1/3}(\alpha)} \quad (31)$$

and with bearings arranged according to shape in the form:

$$K_r = \frac{3 \cdot 10^{-3}}{4} \cdot z^{2/3} \cdot k_\delta^{2/3} \cdot i_1^{2/3} \cdot F_p^{1/3} \cdot \frac{\cos^2(\alpha_1)}{\sin^{1/3}(\alpha_1)} \left[ 1 + \frac{i_2^{2/3} \cdot \cos^2(\alpha_2) \cdot \sin^{1/3}(\alpha_1)}{i_1^{2/3} \cdot \cos^2(\alpha_1) \cdot \sin^{1/3}(\alpha_2)} \right] \quad (32)$$

where the approximate value of the deformation constant is

$$c_\delta = 10^5 \cdot \sqrt{1,25 \cdot d_w} \quad (33)$$

$d_w$  – is the diameter of the balls.

The pre-stressing value “ $F_p$ ” can be calculated according to the standard, STN 02 46 15. Some foreign manufacturers (for example, SKF, FAG, SNFA ...) publish this value in their catalogues. The number of balls “ $z$ ” and their diameters “ $d_w$ ” of some types of bearings are quoted in the literature, e.g. [16].

- Based on the equation for the calculation of a nodal point axial stiffness [17]

$$K_a = \frac{3 \cdot 10^{-3}}{2} \cdot z^{\frac{2}{3}} \cdot k_\delta^{\frac{2}{3}} \cdot i_1^{\frac{2}{3}} \cdot F_p^{\frac{1}{3}} \cdot \sin^{\frac{5}{3}} \alpha_1 \left[ 1 + \frac{i_2^{\frac{2}{3}} \cdot \sin^{\frac{5}{3}} \alpha_1}{i_1^{\frac{2}{3}} \cdot \sin^{\frac{5}{3}} \alpha_2} \right] \quad (34)$$

and substituting the equation in brackets

$$T_1 = 1 + \frac{\frac{2}{i_2^3} \cos^2 \alpha_2 \sin^{1/3} \alpha_1}{\frac{2}{i_1^3} \cos^2 \alpha_1 \sin^{1/3} \alpha_2} \text{ in equation} \quad (35)$$

and

$$T_2 = 1 + \frac{i_2^{\frac{2}{3}} \sin^{\frac{5}{3}} \alpha_2}{i_1^{\frac{2}{3}} \sin^{\frac{5}{3}} \alpha_1} \text{ in equation} \quad (36)$$

the dependence between the axial and radial stiffness can be expressed by the relation

$$K_r = \frac{K_a}{2} \cdot \frac{1}{\operatorname{tg} 2\alpha_1} \cdot \frac{T_2}{T_1} \quad (37)$$

When  $\alpha_1 = \alpha_2$  in a nodal point with bearings arranged according to shape, or  $i = 0$  in nodal points with bearings arranged according to direction, the quotient of the constants  $T_1, T_2$  will be equal to 1 and the relation (37) will be simplified. Thus

$$K_r = \frac{K_a}{2} \cdot \frac{1}{\operatorname{tg} 2\alpha} \quad (38)$$

Taking equations (32) and (34) into consideration, it is evident that the stiffness of the bearing arrangement depends on the number of bearings ( $i_1$  and  $i_2$ ) in the arrangement, the dimensions of the bearings ( $z_1, d_{w1}$  and  $z_2, d_{w2}$ ), the contact angle ( $\alpha_1$  and  $\alpha_2$ ) and the preload value  $F_p$ .

### 3.5. Conclusions of the analysis

The conclusions of the analysis [10] are as follows:

- Radial stiffness increases proportionally with increasing values of "z", "d<sub>w</sub>", "i", "F<sub>p</sub>" and decreases when "a" is prolonged, (Figure 10).
- The parameters "z" and "d<sub>w</sub>" must be evaluated in mutual interaction because they characterize the size and dimensions of the bearings. Increasing both of these parameters, and producing the consequent increase of stiffness of the bearing arrangement, can be achieved by increasing the inner bearing diameter. The disadvantage here is that maximum revolving speed will be reduced. A more suitable solution is to decrease the width of the bearing, e.g. from B72 to B70, B719 or B718. In this case the number of rolling elements "z" will be increased and their diameter "d<sub>w</sub>" will be smaller.
- Considering equations (31), (32) and (34), it is evident that "z" has a more important influence on stiffness than "d<sub>w</sub>". If the diameter of the rolling elements is smaller, their

weight will also be decreased, and this fact will allow an increase in the maximum revolving speed.

- The number of bearings in bearing arrangement "i" is the significant factor which can favourably influence stiffness. But the increased number of bearings will reduce the maximum revolving frequency and therefore it is possible to use this solution only for low speed spindle-bearing systems.
- The preload has a relatively small effect on the stiffness of bearing arrangements. The preload real value also depends on the type of flange used. When fixed flanges are used the preload value can exceed the nominal value by several times. This will cause excessive preload values which produce heat and the bearing arrangement will break down much sooner than expected.
- The contact angle " $\alpha$ " has a significant influence on the variation of the stiffness of the bearing arrangement. When the value of the contact angle is increased, the radial stiffness and maximum revolving speed of the bearing arrangement is also decreased. On the other hand, the axial stiffness of the bearing arrangement will be significantly increased.

#### 4. Optimization of the spindle-bearing system in relation to temperature

In addition to the bearing arrangements, the temperature properties of the bearing supporting node have an increasingly greater significance on the high-speed capability of the bearing. The main goal of this section is to show the SHS design under real operating conditions, taking into consideration the temperature-related behaviour of the spindle and bearing nodes.

The value of the changes in SHS temperature depends on the temperature gradient, the type of bearing arrangement (DB, DF, DT, ...), the contact angle of the bearing, and the distance between the bearings arranged in the node.

The stiffness of the given example was analysed using the application software "*Spindle Headstock*" [3], developed in our department.

The analysis identified the optimal stiffness, which was then applied to the headstock of the DB 24 fy. Ex-Cell-O GmbH., Eislinger precision boring machine, Figure 11, [18]

The headstock used for analysis had the following parameters:

Output power:	$P = 3 \text{ kW}$
Maximum speed:	$n_{c \text{ max}} = 5500 \text{ min}^{-1}$
Shape inaccuracy at boring	$E_s \leq 1,5 \text{ } \mu\text{m}$
Surface roughness:	$E_t = 1 \dots 1,5 \text{ } \mu\text{m}$
Bearings:	FAG B 7016 C.TPA.P4.UL in "O" arrangement
Bearing lubrication:	grease

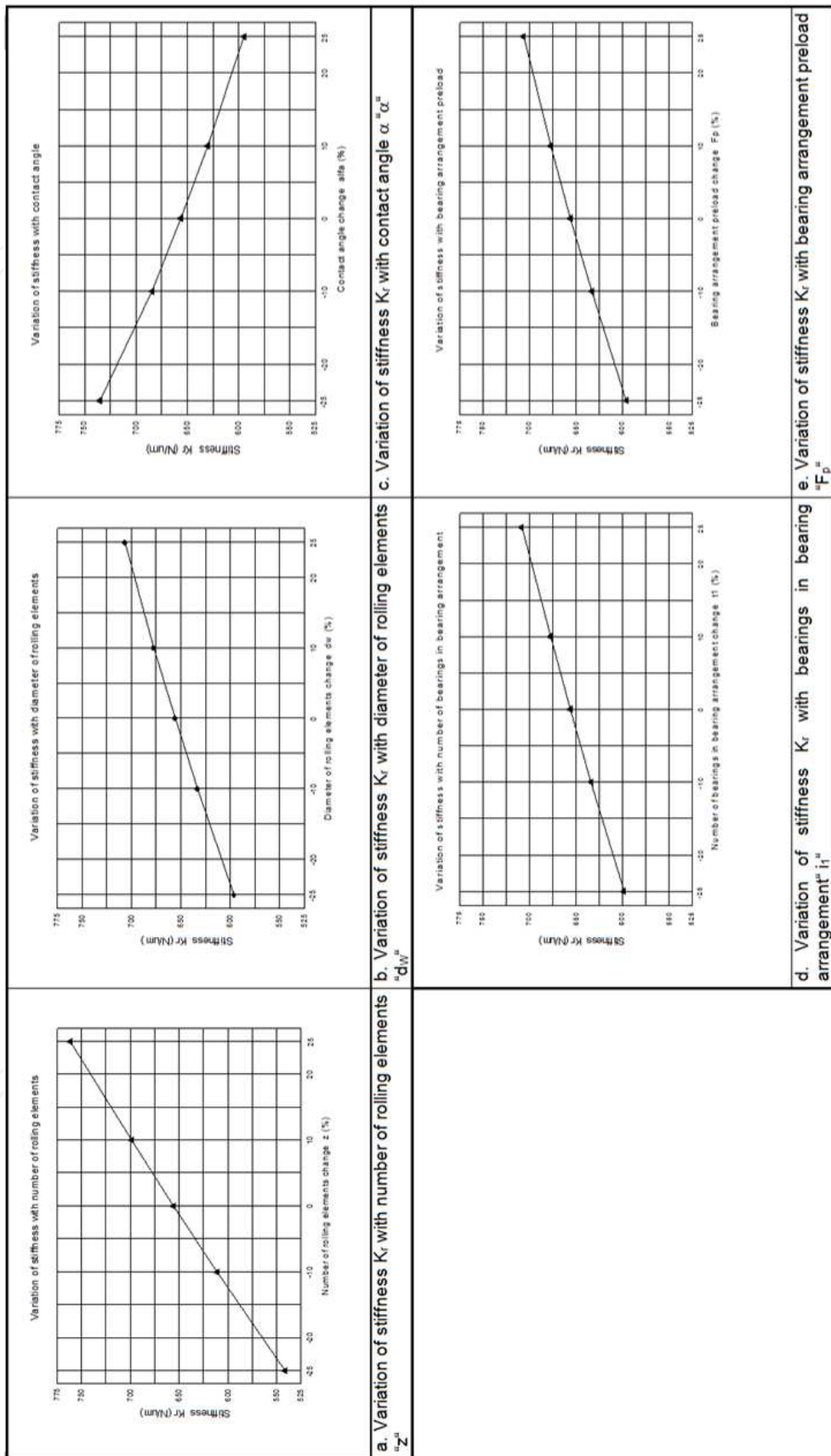
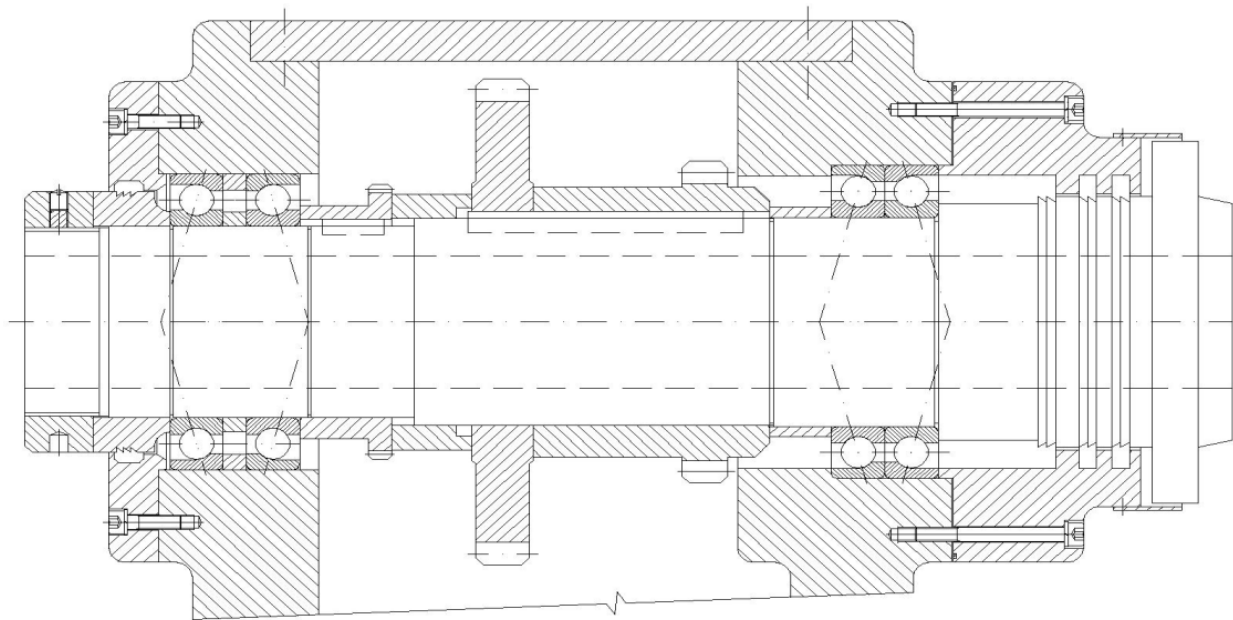
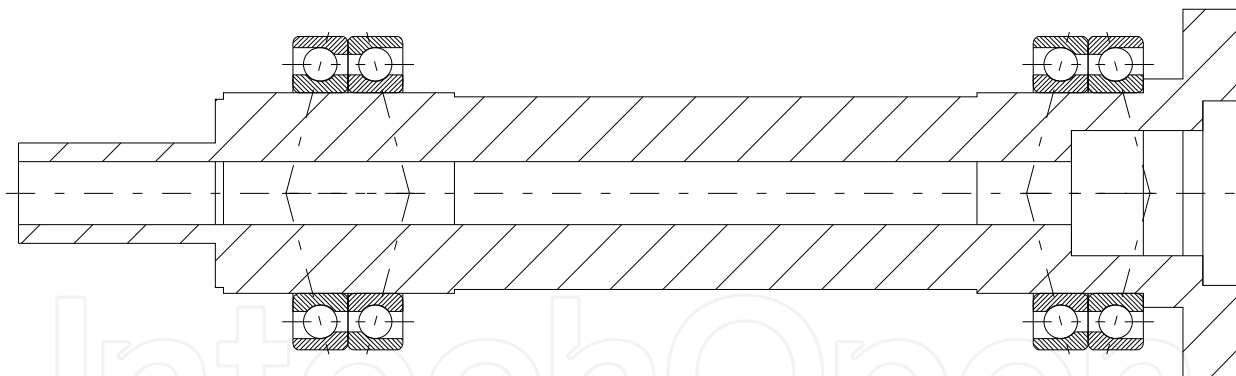


Figure 10. Variation of stiffness with bearing arrangement parameters



**Figure 11.** The Headstock of the precision boring machine DB 24 fy. Ex-Cell-O GmbH., Eislinger, [18]



**Figure 12.** Model of the spindle

Results for spindle with arrangement DB - DB.

Radial load:  $F_r = 1000 \text{ N}$   
 Axial load:  $F_a = 200 \text{ N}$   
 Desired spindle speed:  $n_{ot} = 5500 \text{ min}^{-1}$   
 No driving force  
 Working conditions  
 Lubrication: Plastic grease  
 Cooling: Good cooling

	Rear support	Front support
<b>Bearings</b>		
- type:	2pc. [B 7016 CTB]	2pc. [B 7016 CTB]
- dimensions [mm]:	D= 125 d= 80 B= 24 dW=13.49	D=125, d=80, B=24, d <sub>w</sub> =13.49
- arrangement:	◇	◇
- precision grade:	P4	P4
Preload:	Light	Light
Flange:	Fixed flange	Fixed flange
Maximum speed:	Z <sub>nmax</sub> = 5 256 min <sup>-1</sup>	Z <sub>nmax</sub> = 5 256 min <sup>-1</sup>
Pre-load:	ZF <sub>p</sub> = 404 N	PF <sub>p</sub> = 402 N
Reactions:	R <sub>A</sub> = 205 N	R <sub>B</sub> = 1 205 N
Radial stiffness:	K <sub>rA</sub> = 666 243 Nmm <sup>-1</sup>	K <sub>rB</sub> = 651 216 Nmm <sup>-1</sup>
Axial stiffness:	K <sub>aA</sub> = 97 860 Nmm <sup>-1</sup>	K <sub>aA</sub> = 97 745 Nmm <sup>-1</sup>
Durability:	T <sub>rvZ</sub> = 394 366 hours	T <sub>rvP</sub> = 225 577 hours
Bearings distance:	L = 297 mm	
Total displacement at the end:	y <sub>r(L+a)</sub> = 0.00372931 mm	
<b>Total stiffness:</b>	<b>K<sub>rc</sub> = 268 146 Nmm<sup>-1</sup></b>	
<i>Optimal calculated values</i>		
Optimal bearing length:	L <sub>opt</sub> = 283.6 mm	
Optimal displacement at the end L <sub>Opt</sub> :	y <sub>rmin</sub> = 0.00372686 mm	
<b>Optimal stiffness:</b>	<b>K<sub>rcopt</sub> = 268 322 Nmm<sup>-1</sup></b>	

#### 4.1. The optimisation of SHS with regard to temperature

The temperature dilatation of the spindle can be described by the equation:

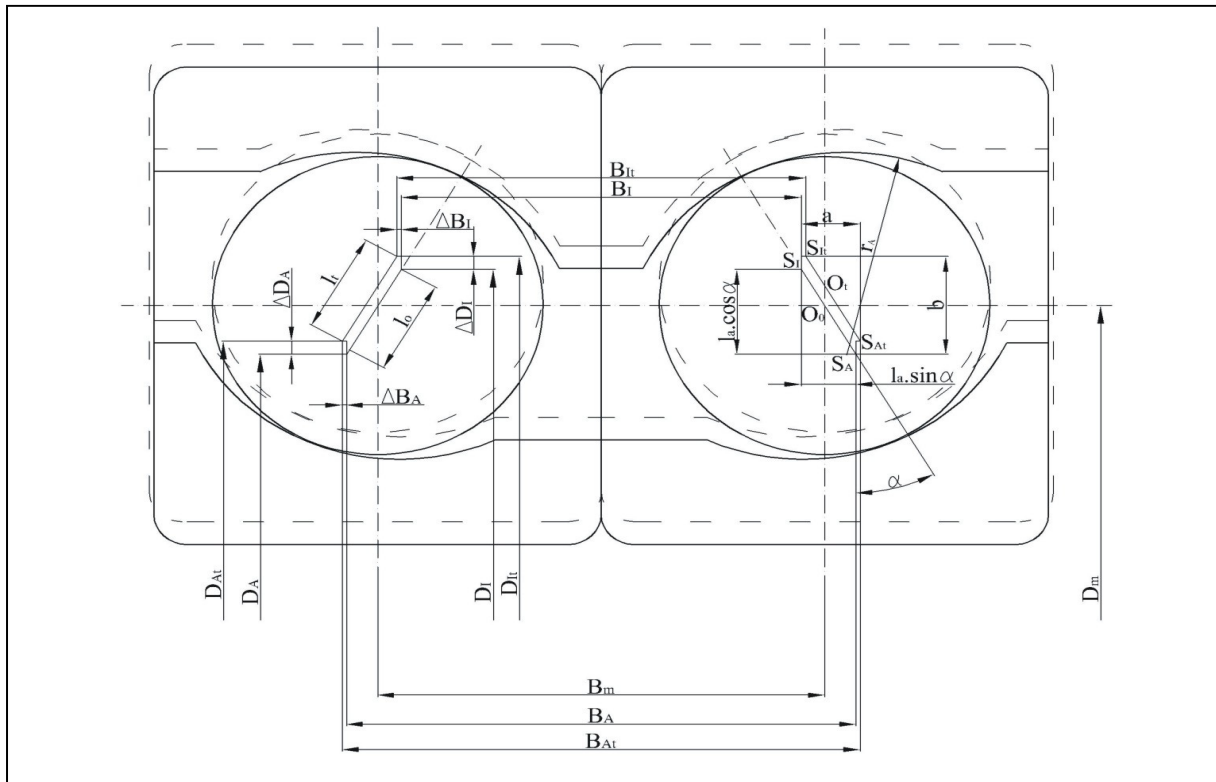
$$\Delta L = \lambda_t \cdot L \cdot \Delta t \quad (39)$$

If the distance between the bearings in the "DB" arrangement is short (Figure 13a), the dilatations in a radial direction is greater, [18]. The temperature gradient causes the dilatation of the inner bearing rings to be greater than that of the outer rings. Consequently, the original preload increase in temperature will be higher in the bearing node. The elevated temperature will influence the temperature gradient, and the preload value could cause bearing node failure.

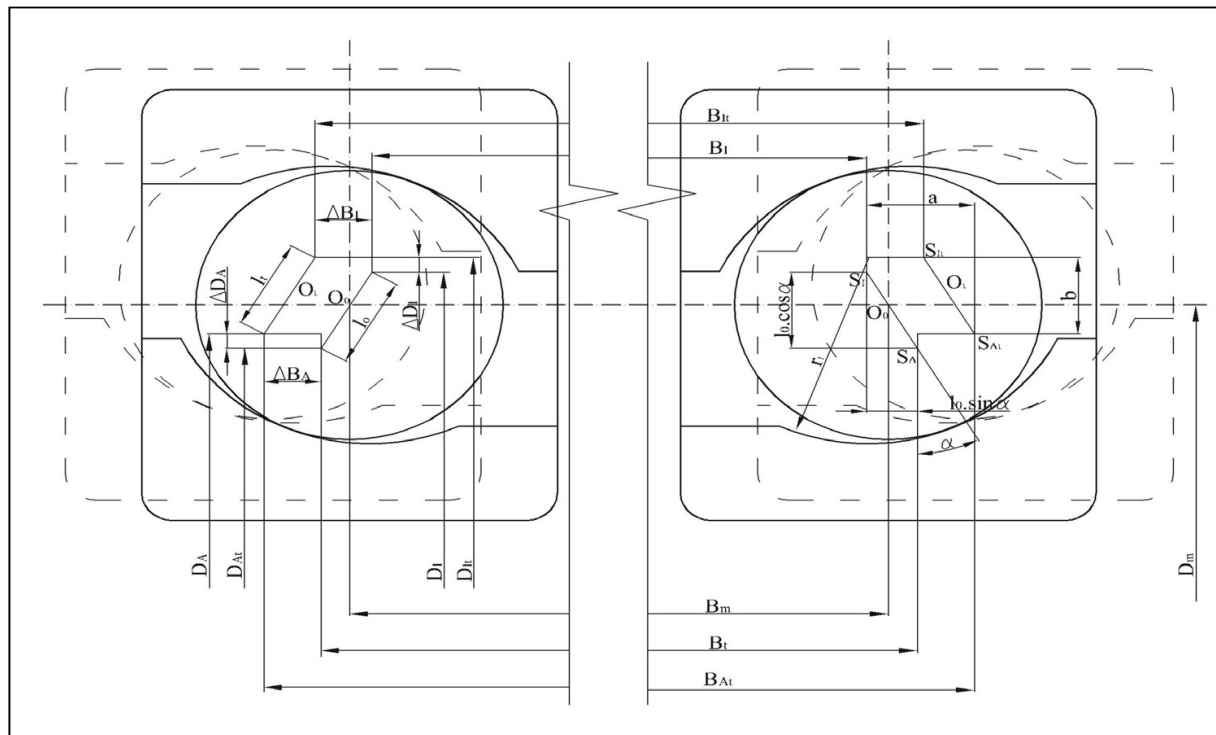
The preload change was defined by the change in the distance between the centres of the radii of the rolling raceways:

$$l_0 = r_A + r_I - d_w \quad (40)$$

The distance  $l_t$  at given temperature gradient in accordance with Figure 13 is



a) Distance between bearings  $B_m = 29 \text{ mm}$



b) Distance between bearings  $B_m = 500 \text{ mm}$

**Figure 13.** Temperature deformation of bearing arrangement B 7016 C TPAP4UL in "DB"

$$l_t = \sqrt{a^2 + b^2} \quad (41)$$

where

$$a = l_0 \cdot \sin \alpha + \frac{\lambda_t}{2} \cdot [B_m \cdot (t_I - t_A) + l_0 \cdot \sin \alpha \cdot (t_I + t_A - 2 \cdot t_0)] \quad (42)$$

$$b = l_0 \cdot \cos \alpha + \frac{\lambda_t}{2} \cdot [D_m \cdot (t_A - t_I) + l_0 \cdot \cos \alpha \cdot (t_I + t_A - 2 \cdot t_0)] \quad (43)$$

The magnitude of deformation will be

$$\Delta \delta = l_0 - l_t \quad (44)$$

and preload change in accordance with [18] will be

$$\Delta F = \Delta \delta \cdot z^{2/3} \cdot c_\delta^{2/3} \cdot \sin^{8/3} \alpha \quad (45)$$

where

$$c_\delta = 10^5 \cdot \sqrt{1,25 \cdot d_w} \quad (33)$$

In the twin bearings FAG B 7016 C.TPA.P4.UL with "DB" arrangement, at a temperature gradient of 10 °C, and with bearing distance  $B_m = 29$  mm, the preload will increase by 13,32 N.

Conversely, if the distance of the bearing in "O" arrangement is long (Figure 13b), the dilatations in the axial direction prevail and cause a decrease in the value of the preload.

In the twin bearings FAG B 7016 C.TPA.P4.UL with "DB" arrangement, at a temperature gradient of 10°C, the preload will be decreased by 5,88 N.

In "DB" arrangement, the main goal of temperature optimization is dependant on the determination of the optimum distance between the bearings at which a change in the preload at the given temperature gradient would be minimal.

In accordance with Figure 13 the condition

$$l_0 = l_t \quad (46)$$

must be satisfied.

By substituting equations (42) and (43) into (46), the optimal bearing separation distance from the point of view of temperature can be deduced from:

$$B_{mopt} = D_m \cdot \frac{\cos \alpha}{\sin \alpha} - \frac{l_0 \cdot (t_I + t_A - 2 \cdot t_0)}{t_I - t_A} \cdot \left( \frac{1}{\sin \alpha} \right) \quad (47)$$

Figure 14 shows the change of optimal bearing distance at various values of the temperature gradient for the analysed SBS, Figure 11.

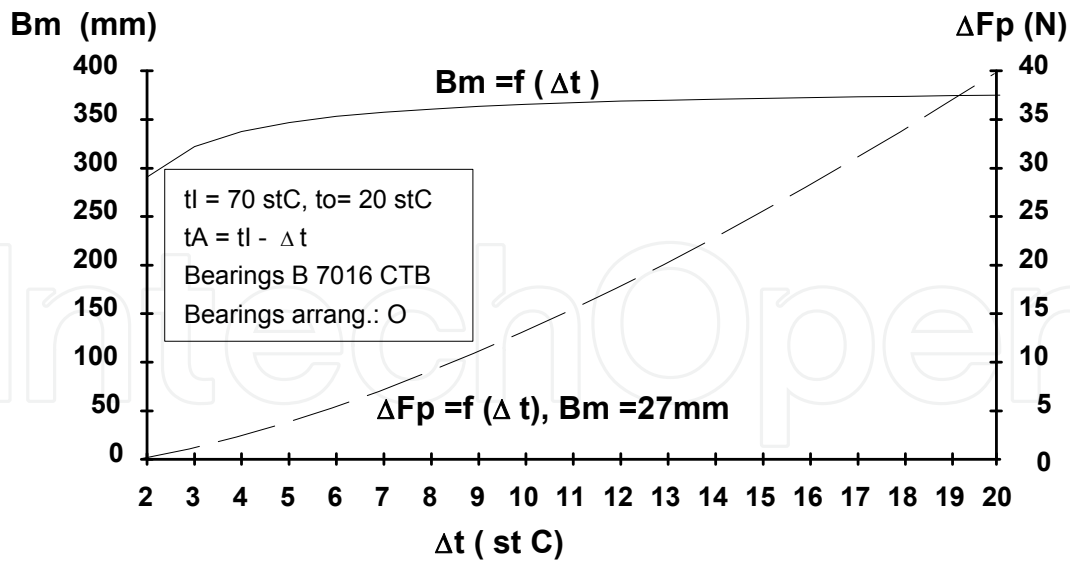


**Figure 14.** The inter - dependence of bearing preload change, ideal distance between bearings and change of temperature in the bearings arrangement system.

#### 4.2. Recommendation for improvements in construction

The recommendations from the point of view of temperature optimisation for the DB 24 SHS boring machine are based on the results of the analysis undertaken. From the perspective of temperature, it can be seen that a change in bearing node arrangement to individual spindle supports from "DB" to "DT" would be advantageous, Figure 15.

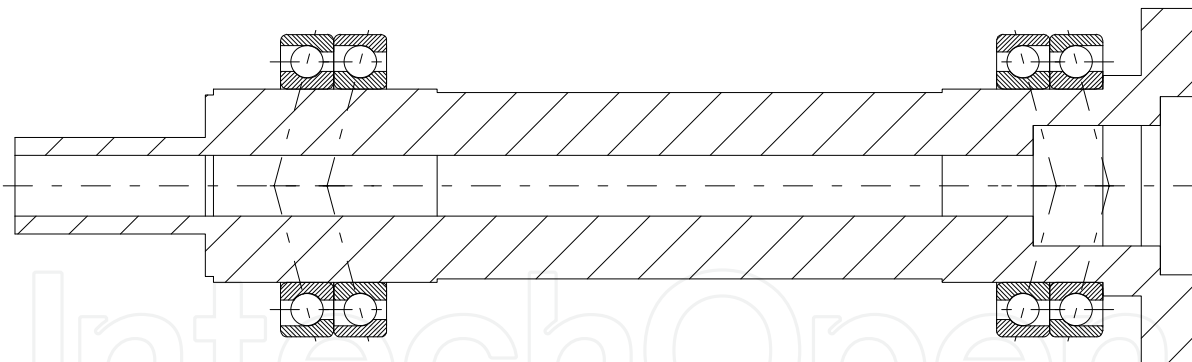


**Figure 15.** Model of the spindle

Results for spindle with arrangement DB - DB.

Radial load:	$F_r = 1000 \text{ N}$
Axial load:	$F_a = 200 \text{ N}$
Desired spindle speed:	$n_{ot} = 5500 \text{ min}^{-1}$
No driving force	

*Working conditions*

Lubrication:	Plastic grease
Cooling:	Good cooling

	<b>Rear support</b>	<b>Front support</b>
Bearings		
- type:	2pc. [B 7016 CTB]	2pc. [B 7016 CTB]
- dimensions [mm]:	D= 125 d= 80 B= 24 dW=13.49	D=125, d=80, B=24, dW=13.49
- arrangement:	◇	◇
- precision grade:	P4	P4
Preload:	Light	Light
Flange:	Fixed flange	Fixed flange
Maximum speed:	$Z_{n_{max}} = 5\ 256\ \text{min}^{-1}$	$Z_{n_{max}} = 5\ 256\ \text{min}^{-1}$
Pre-load:	$ZF_p = 404\ \text{N}$	$PF_p = 402\ \text{N}$
Reactions:	$R_A = 205\ \text{N}$	$R_B = 1\ 205\ \text{N}$
Radial stiffness:	$K_{rA} = 666\ 243\ \text{Nmm}^{-1}$	$K_{rB} = 651\ 216\ \text{Nmm}^{-1}$
Axial stiffness:	$K_{aA} = 97\ 860\ \text{Nmm}^{-1}$	$K_{aA} = 97\ 745\ \text{Nmm}^{-1}$
Durability:	$T_{rvZ} = 394\ 366\ \text{hours}$	$T_{rvP} = 225\ 577\ \text{hours}$

Bearings distance:	$L = 297\ \text{mm}$
Total displacement at the end:	$y_{r(L+a)} = 0.00372931\ \text{mm}$
<b>Total stiffness:</b>	<b><math>K_{rc} = 268\ 146\ \text{Nmm}^{-1}</math></b>

#### *Optimal calculated values*

Optimal bearing length:	$L_{opt} = 283.6\ \text{mm}$
Optimal displacement at the end $L_{Opt}$ :	$y_{rmin} = 0.00372686\ \text{mm}$
Optimal stiffness:	$K_{rcopt} = 268\ 322\ \text{Nmm}^{-1}$

In comparison with the original bearing node arrangement, the radial stiffness of the rearranged spindle-bearing system will drop slightly, but its axial stiffness will increase. The advantage of the reconfigured SBS is that at real mean values of temperature gradient, the SBS stiffness will be almost fixed.

### **4.3. Spindle headstock**

The application software is used for calculating the SBS of machine tools supported on rolling bearings. The programme enables us to determine all elements and calculate the properties of the spindles and shafts which are supported on rolling bearings. The application software enables very fast and user-friendly calculation of the radial spindle stiffness in the bearing arrangement in a bearing unit.

The architecture of the programme contains a number of mathematical formulae which have been experimentally verified. These models respect the conditions of the spindle working accuracy in terms of the external load cutting forces, driving forces, and also spindle rotation speed.

#### **The basic interactive programme offers:**

1. The ability to input user-determined conditions for the calculation and optimisation of the spindle fitting system (Figure 16);

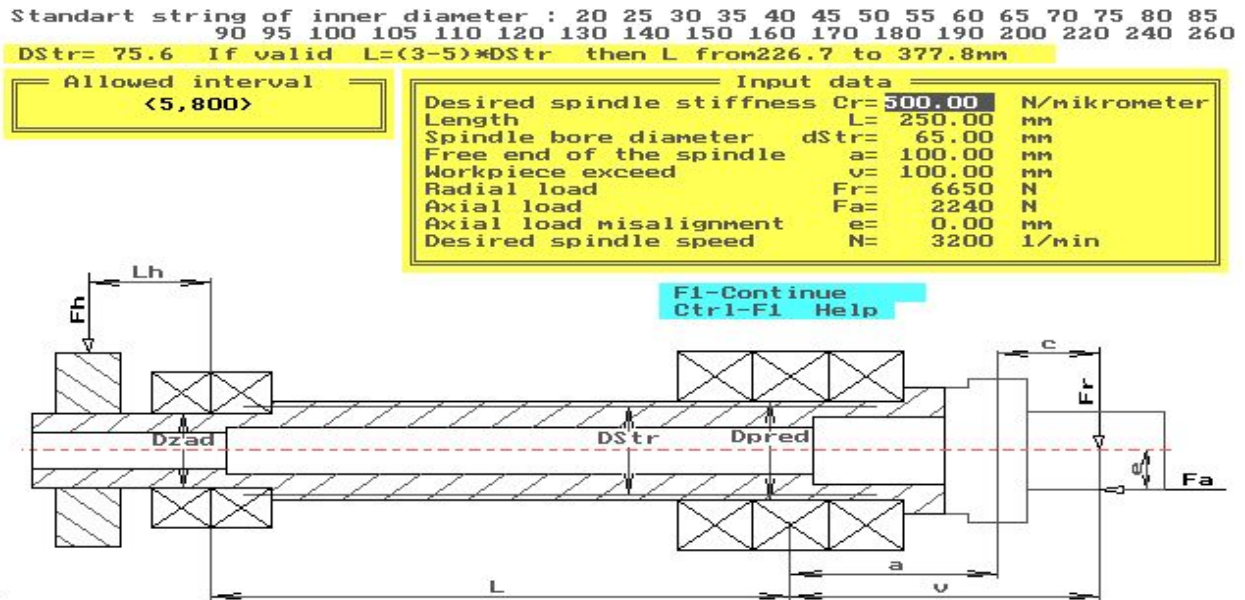


Figure 16. Entering the input data

2. The ability to select the most appropriate bearing or bearing node arrangements (Figure 17, Figure 18, Figure 19). Data about selected bearings can be ganged from extensive databases according to the users requirements within the bearing inner diameter range:

- angular contact ball bearings, type 7 10..150 mm
- single row cylindrical roller bearings, type N 50..120 mm
- full cylindrical roller bearings, type NN 30..440 mm
- axial angular contact bar, type 2344 25..380 mm
- thrust ball bearings, single direction, type 51 10..360 mm
- thrust ball bearings, double direction, type 52 10..190 mm
- deep groove ball bearings, type 6 3..360 mm;

### Variant selection: \* Front support \*

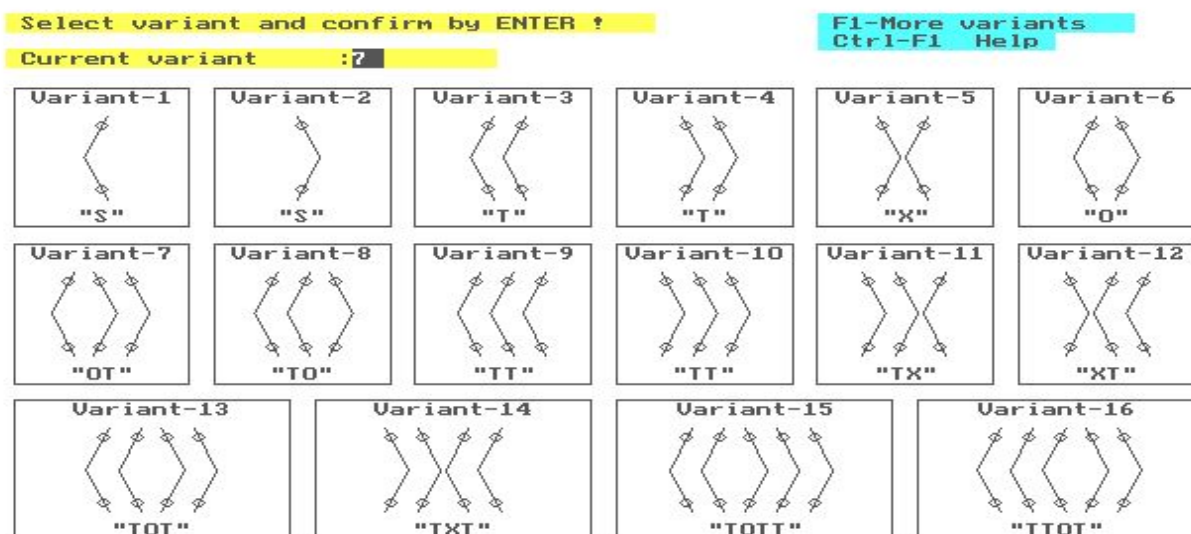


Figure 17. Selection of the bearing arrangement and type of bearings

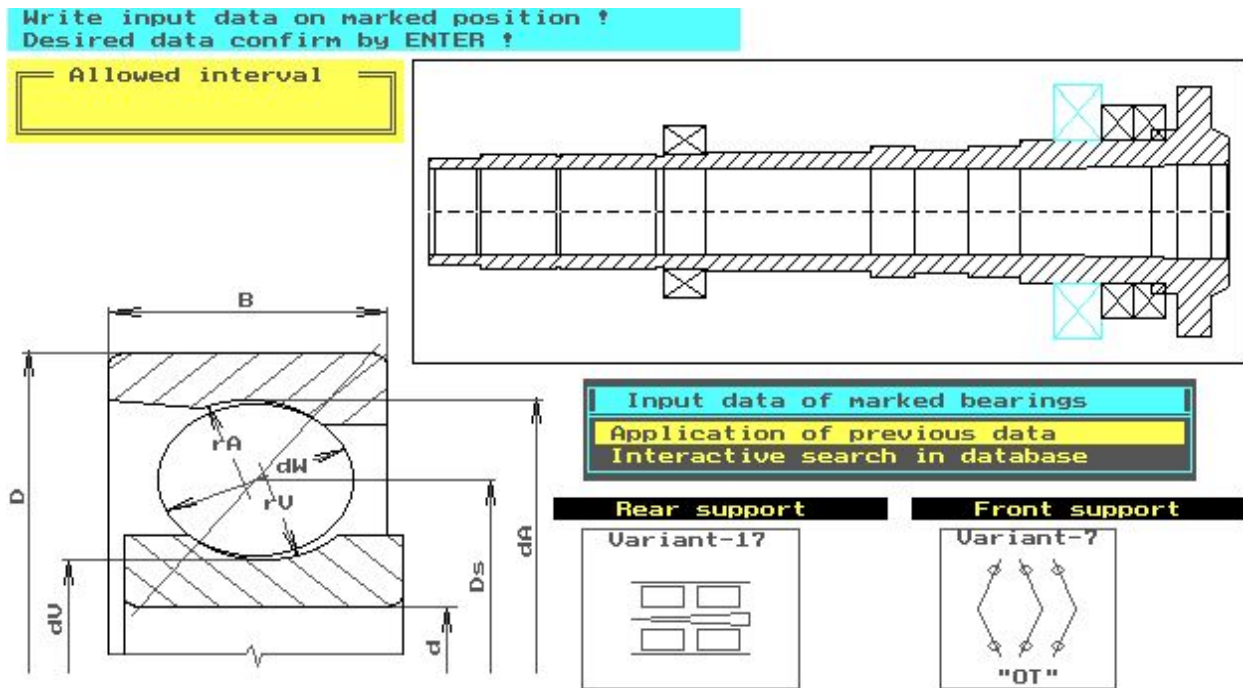


Figure 18. Dimensional design data of the spindle housing

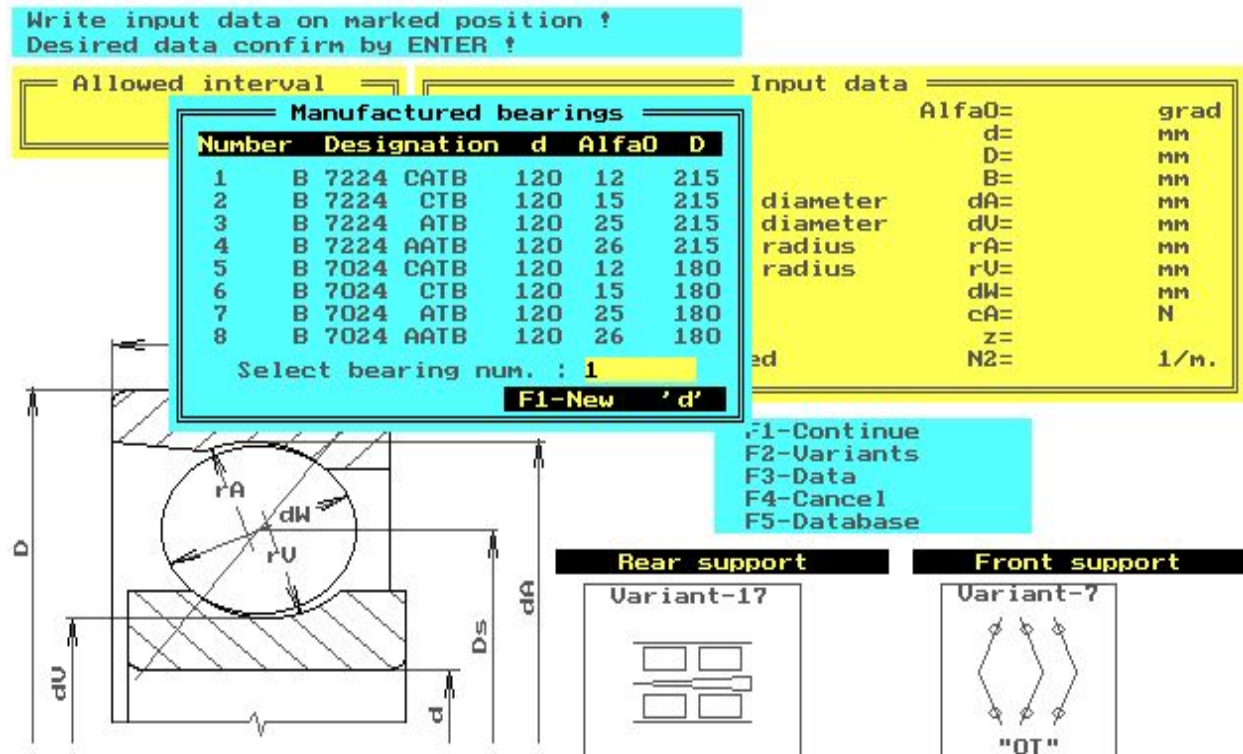


Figure 19. Changing data of the bearings mounting

3. The identification and selection of the standardized spindle nose for turning, milling, grinding and boring;
4. The choice of the design parameters and spindle suitability for different working conditions (working accuracy, preloading, flange type, lubrication system, cooling), Figure 20;



**Figure 20.** Entering preliminary data for the bearings conditions

5. The calculation and optimization of the cutting parameters for the required material to be machined (cutting force, torque, feed, power), Figure 21;
6. Calculation and optimization of the design and fitment with regard to the applied conditions (revolving speed, radial stiffness, axial stiffness, rating life) for the bearing units and the fitting as a whole, for all of the identified bearing types.

Graphical output of partial deflections caused by bearing nodes distance are shown in Figure 21.

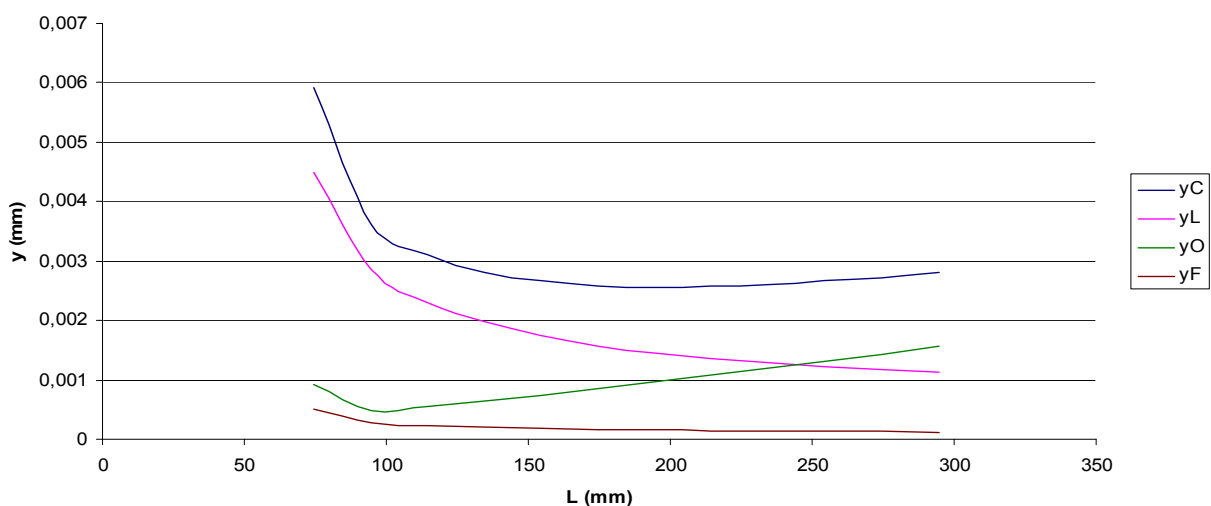


**Figure 21.** Graphical output of the dependence of partial deflection on bearing node distance

The results include:

- applied entries
- chosen bearing (unit) fit types
- rotational speed limit
- radial unit stiffness

- axial unit stiffness
- resultant stiffness for the chosen spindle fit system
- load parameter and durability
- graphical illustration of the chosen design (Table 1.).

The "Spindle Headstock" software application product is a basic programme which can be modified according to the user's wishes.

The programme has been written in the source code programming language, T-PASCAL v.7, with special additional modules for graphics. A number of interactive modules prepare user-specified data for use in AutoCAD utilising the DXF format. The programme can be used on any IBM/PC compatible computer using a HERCULES, EGA or VGA graphics adapter.

The applied software technology has been used in the industry to improve the working accuracy of the machine tools made by TOS Trenčín-Slovakia, for SN and SPSI type lathes , (2), and to design the boring headstocks for the modular single-purpose machine tools made by TOS Kuřim-Czechoslovakia, (5) TOS Lipník, SKF, GMN and INA Skalica. The programme is very effective and reliable and comparison of the results between experiments and calculations show good correlation, never exceeding 10 %.

## 5. Experimental research

Theoretical results and hypotheses must be verified by experimental tests.

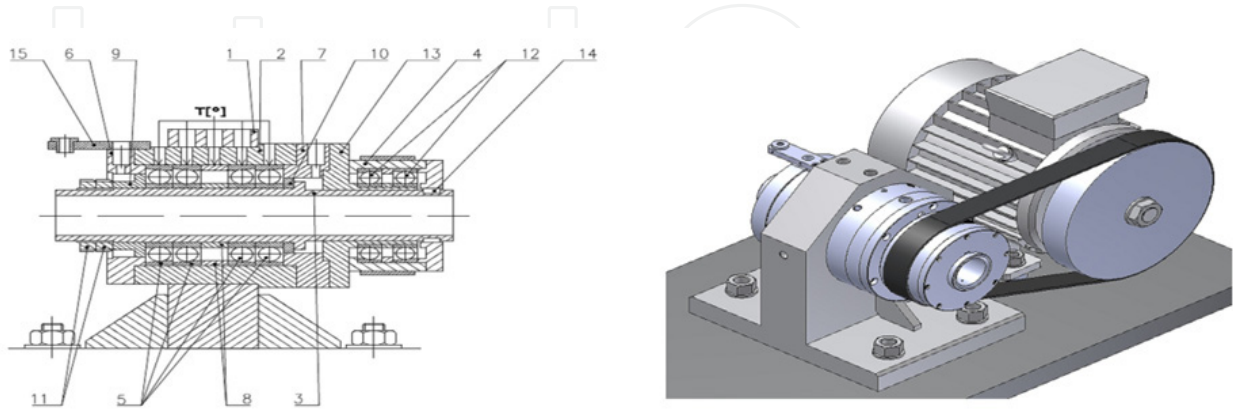
### 5.1. Research of bearing nodes characteristics

In some cases it is very difficult, or even impossible, to gain experimental results from actual machine tools. This led us to develop an experimental device for research into spindle bearing node arrangement characteristics. Our department has developed such a device that can measure:

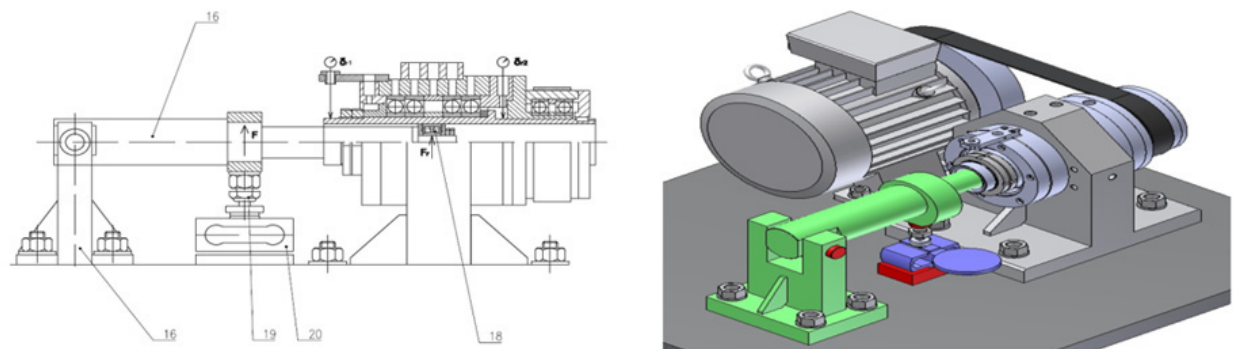
1. changes in the bearing contact angle at its mounting point, changes in loading, and changes in revolving frequency,
2. deformation from axial and radial loading for various preload arrangements, contact angles and bearing node revolving speed settings
3. increases in the temperature in the bearing nodes at various settings
4. dimension of cutting forces in bearing nodes

The variation in the stiffness of the bearing arrangement B7216 is shown in Figure 22, [19]. We can use the experimental measuring head for measuring the deflection and temperature of a varying number of bearings and bearing nodes (from 2 to 5), their preload value, dimensions, and the contact angle of the bearings with different radial and axial forces used, [19], [20].

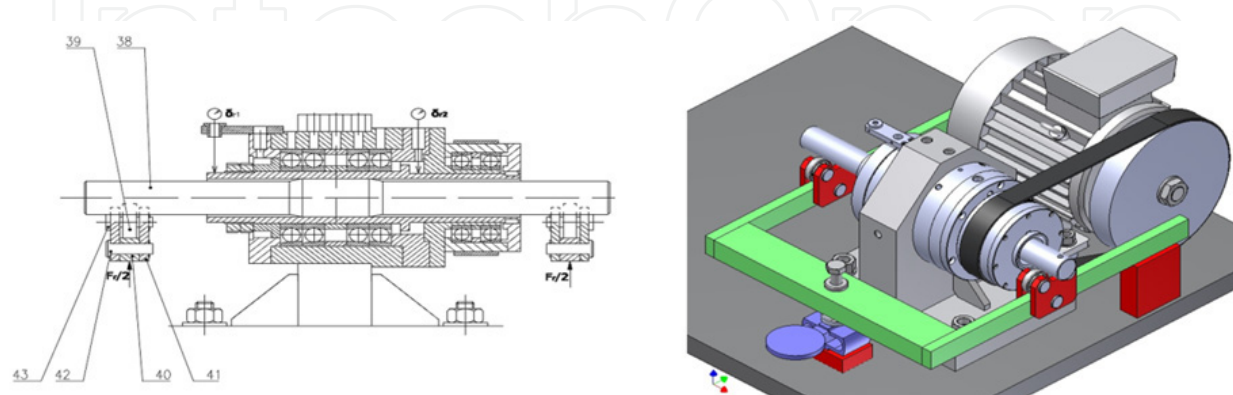
We use this device to measure the deformation characteristics of the bearing node with different combinations of bearing arrangement, pre-stressed values, contact angles, loads and revolution frequencies. We use this experimental measuring head for verifying the theoretical calculation and real performances of the bearing node (stiffness, precision running and temperature).



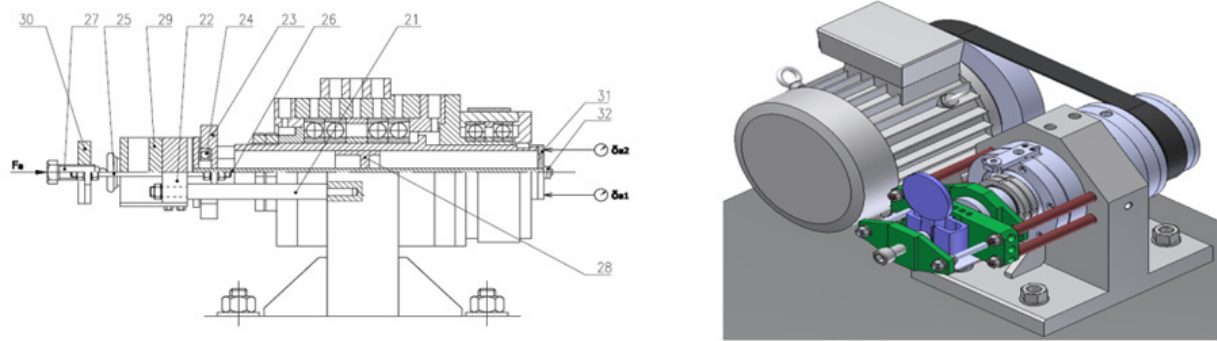
a) cross section of the experimental measuring head with driver, 1- head, 5-bearing node, 4- band wheel



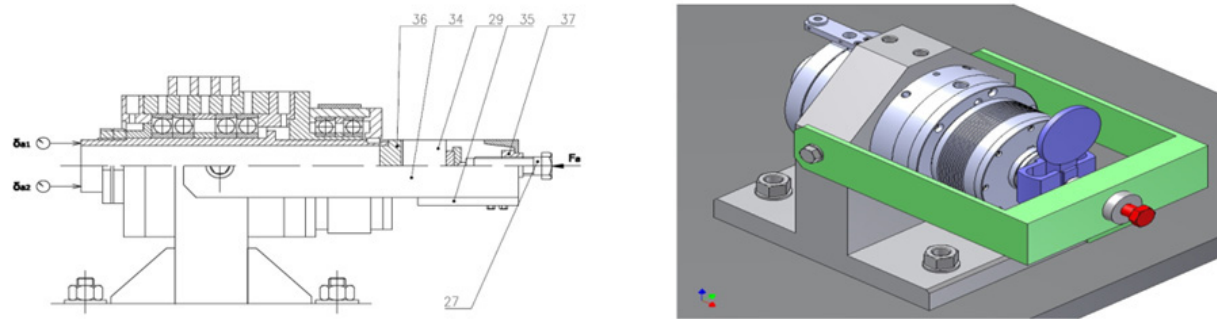
b) arrangement of experimental measuring head for measuring radial stiffness by spindle speed 16 - holder, 19 - tightening screw, 20 - dynamometer, 18 - force bearing



c) arrangement of experimental measuring head for measuring precision running and temperature by spindle speed, 43 - force bearing



d) arrangement of experimental measuring head for measuring radial stiffness by spindle speed with, 22 - holder, 27 - tightening screw, 29 - dynamometer, 24 - force bearing, 32 - flange



e) arrangement of experimental measuring head for measuring static axial deflection and temperature, 34 - holder, 27 - tightening screw, 29 - dynamometer

**Figure 22.** Different variants of the experimental measuring head

In Figure 23 we have compared the experimental stiffness measurement, with the accurate theoretical and simplified average calculated radial stiffness of the B7216 AATBP4OUL bearing arrangement. The stiffness variation was examined with a 25% contact angle with nominal value of bearing arrangements:  $z_1, z_2 = 14$ ,  $d_{w1}, d_{w2} = 19,05$  mm,  $\alpha_1, \alpha_2 = 12^\circ$ ,  $F_p = 340$  N.

When static, the experimental values of radial stiffness are higher than the theoretical values. The dependence of stiffness on loading exhibits a decreasing pattern. The decrease is nearly linear, until a certain critical force " $F_{kr}$ " is reached, at which point the roller with the lightest load becomes unloaded. The deformation characteristic of the nodal point is influenced by the type of flange. The degree and gradation of the stiffness change under the given operational conditions depend on their construction.

In this field the results of the precise and the approximate mathematical model are practically the same. Consequently it follows that in a preliminary mounting design, a simplified mathematical model for calculating the stiffness of the nodal points can be used, as suggested in this article. The convergence of the measured and calculated values provides good evidence for a wider application of the programme in practice.

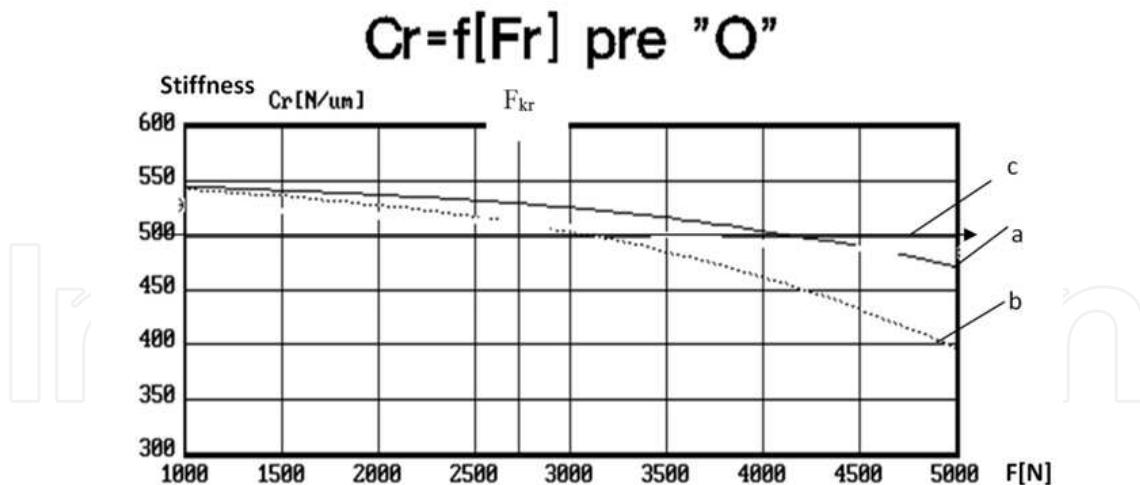


**Figure 23.** Radial stiffness of the bearing arrangement B7216 AATB P4 O UL, a - experimental, b - accurate theoretical c- simplified average

## 5.2. New design of headstock

In the new design of a headstock which connects to a CNC system, the maximum width of cut is limited by the point at which self-exciting vibration starts.

From a constructional point of view, the headstock design can be classified as follows:

- classical headstock
- headstock with an integrated drive unit

The classical headstock is a mechanical unit, where a spindle is driven by a motor through a gearbox without any control system.

The disadvantages of the classical construction are as follows:

- problems with the gears at higher revolving frequencies,
- actual cutting speeds are not continual because of the discontinuous nature of the gearboxes,
- large dimensions of complete units

### New design "Duplo-Headstock"

The "Duplo-headstock" has been designed in order to achieve technological parameters comparable to the performance of standard electro-spindles, but at a lower production costs and with higher controllability. This particular headstock is assembled from readily available elements (bearings, single drives,). The demands on the other peripheral devices are reduced, as are the costs.

The "Duplo-headstock" can be described as a spindle with double supports, driven by two separate motors which can operate independently or together. Figure 24 - 28 show a „Duplo-headstock“ design [20].

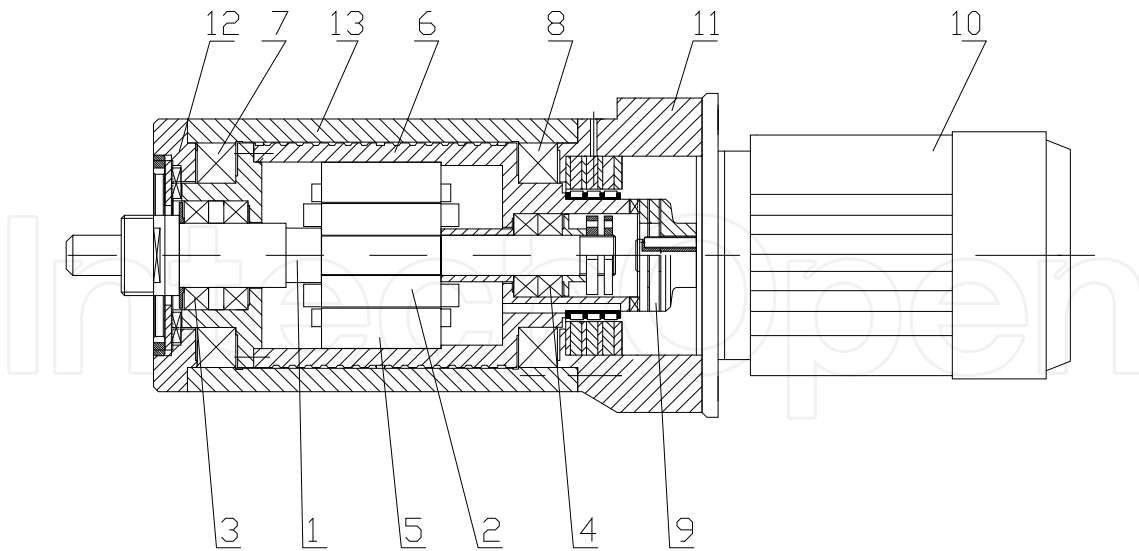


**Figure 24.** High-speed headstock "Duplo"

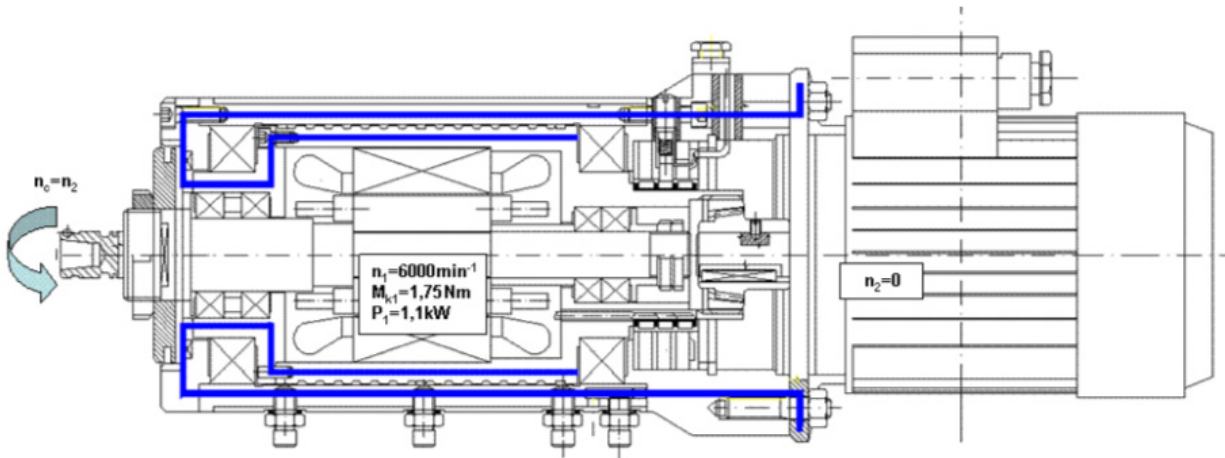


**Figure 25.** The stator engaged on spindle, Speed:  $n_{1max}=6000$  (min-1);  $n_2=0$ ,  $n_{c\_spi}=n_1$  Torque moment:  $M_{k\_sp}=M_{k1}=1,75$  (Nm) by  $n_{1max}$ , Power:  $P_{c\_sp}=P_1=1,1$  (kW)

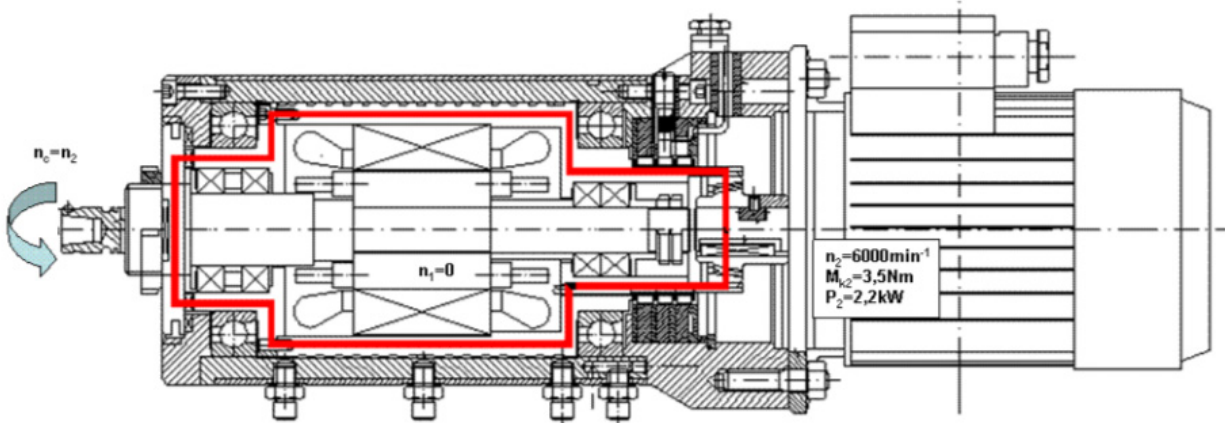


**Figure 26.** The stator engaged on body, Speed:  $n_{1max}=0$ ;  $n_2=6000$  (min-1),  $n_{c\_sp}=n_2$ , Torque moment:  $M_{k\_sp}=M_{k2}=3,5$  (Nm) by  $n_{2max}$ , Power:  $P_{c\_sp}=P_2=3,5$  (kW)

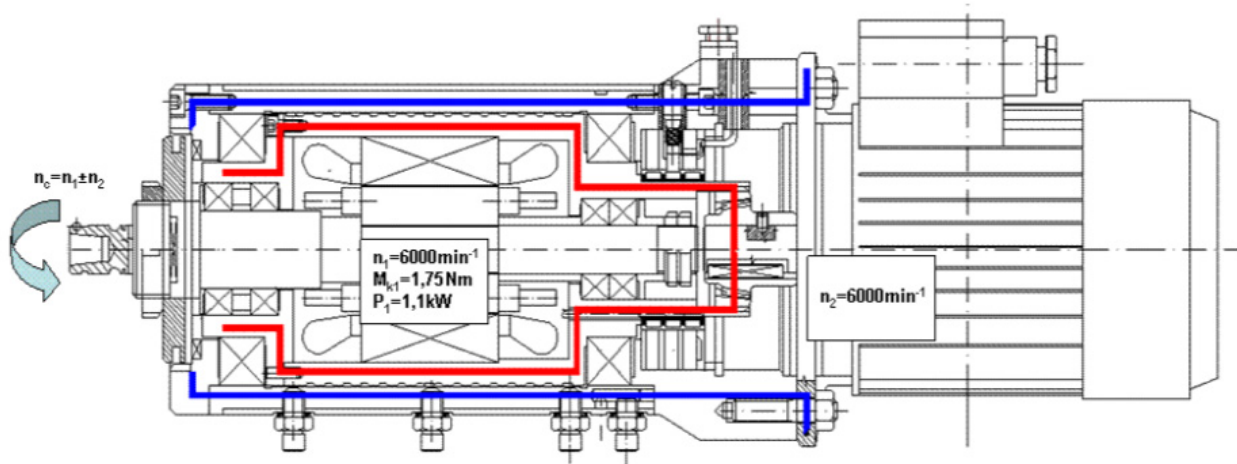


**Figure 27.** Disengaged, Speed:  $n_{1max}=6000$  (min-1);  $n_2=6000$  (min-1),  $n_{c\_sp} = n_1 + n_2$  by one direction of rotation,  $n_{c\_sp} = n_1 - n_2$  by opposite direction of rotation, Torque moment:  $M_{k_{c\_sp}}=M_{k_1}=1,75$  (Nm) by  $n_{1max}$ , Power:  $P_{c\_sp}=P_1=1,1$  (kW)

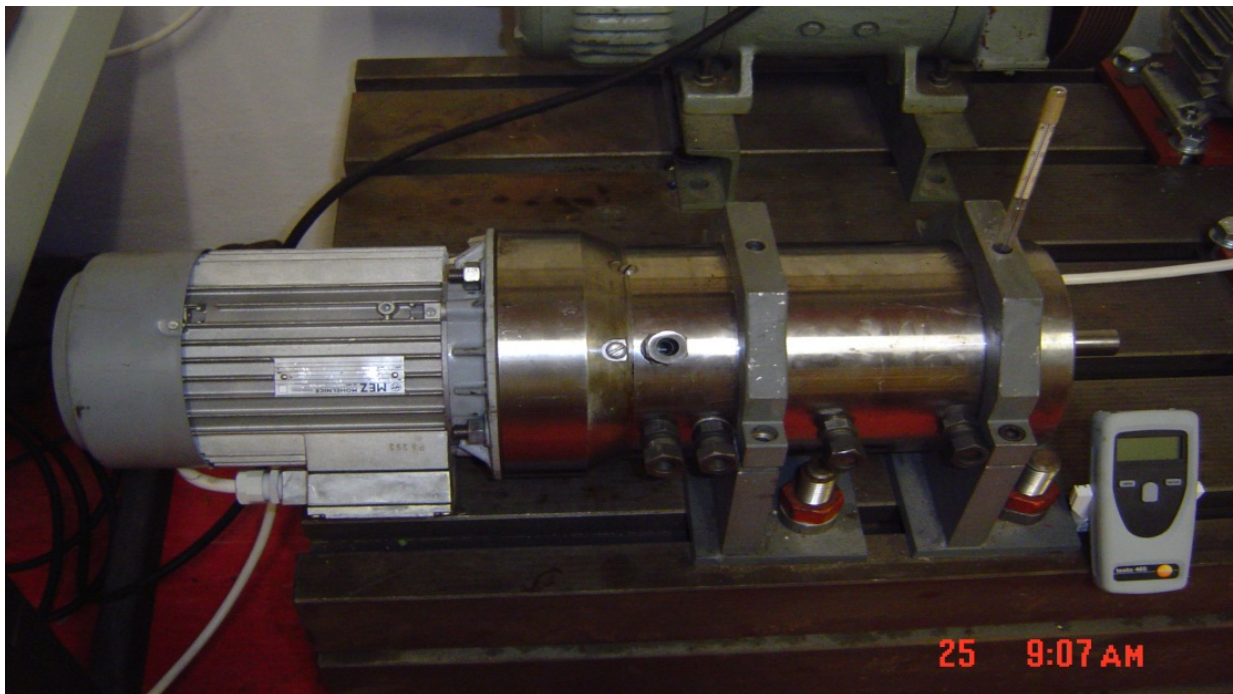


**Figure 28.** Stand of "Duplo" Headstock

The spindle (1), with built-in armature (2), is supported by bearings (3), (4). The stator of the internal motor (5) is supported on bearings (7), (8). The clutch (9) connects a hollow shaft with an external electro-motor (10). The stator feeding rings (11) are located in the rear part of the shaft. The clutch (12) enabling switching between working modes is located in the front part of the shaft. The advantage of this innovative design, which is already in use, is that the headstock can work in three different modes:

- stator is engaged on the spindle
- stator is engaged on the body
- no engagement

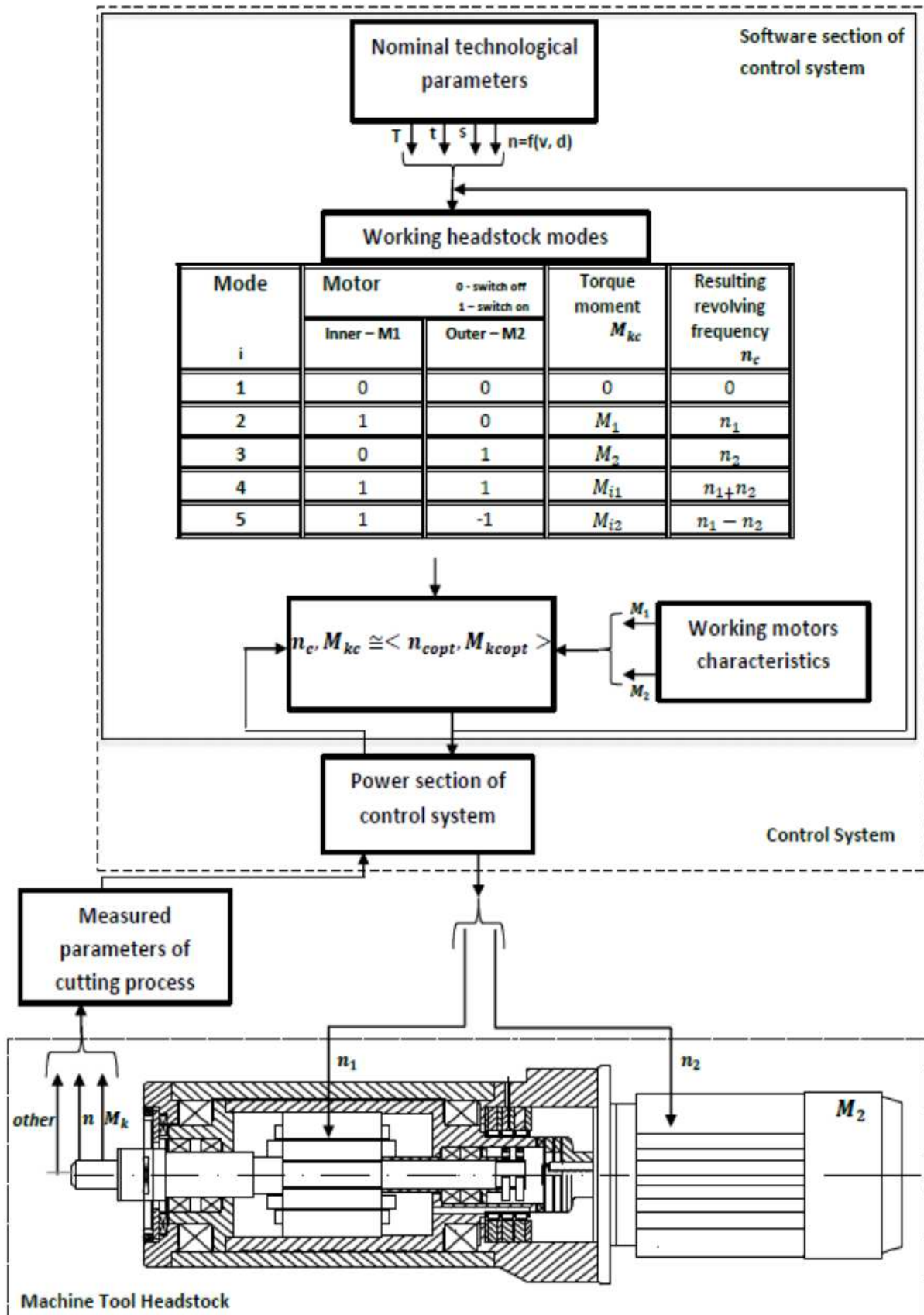
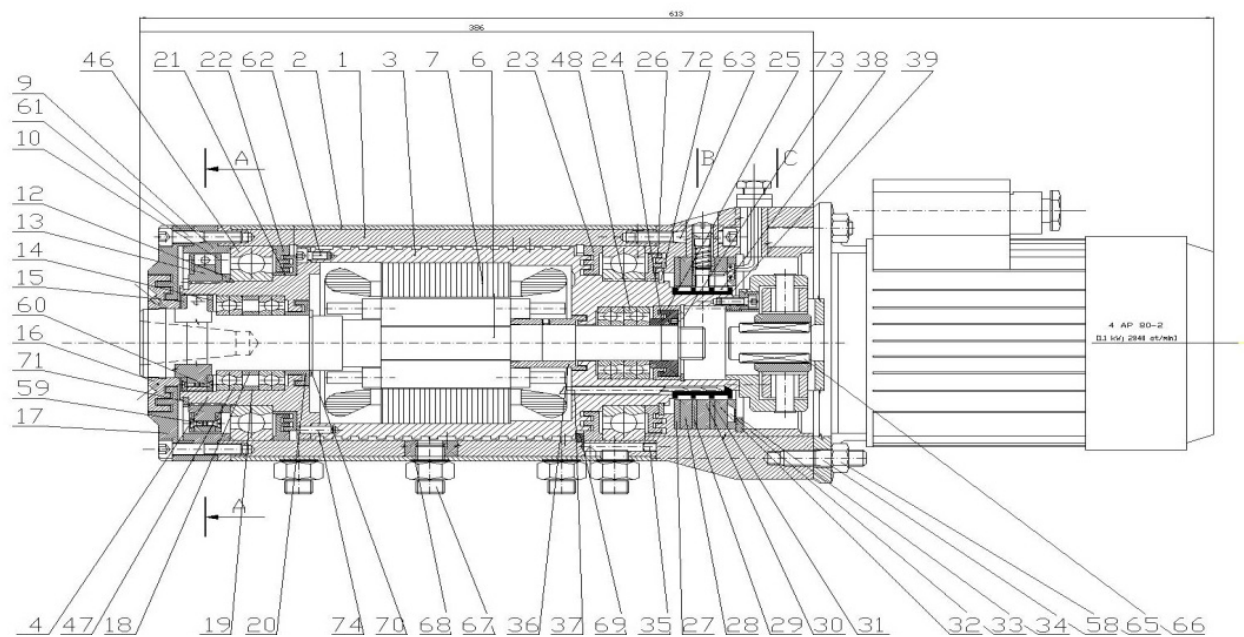


Figure 29. Scheme of Machine Tool Headstock Control

Connecting such a headstock with a suitable control system can provide optimal cutting conditions for various technological operations. The intelligent control system, Figure 29, can operate in any one of the working modes and ensure nominal or optimal technological parameters best suited to the machining process, [21]. Figure 30 shows the design for the construction of the "Duplo" Headstock.

In the third mode, the clutch (12) is switched off. The spindle (1) is driven by both motors, (Figure. 27), providing the maximum speed, which is required, for example, in grinding.



**Figure 30.** Design for the construction of "Duplo" Headstock

## 6. Application research

### 6.1. The new headstock construction for turning machine tools

TRENS a. s. Trenčín, is a Slovak manufacturer of machine tools (mainly lathes) and offers a new generation of lathes implementing various technological advances in design, production, and control systems, [22]. The Department of Production Engineering has been asked to design an accurate running spindle for the SBL 500 CNC lathe (Figures 31 -33), [23]. All construction data and results of measurements were obtained from the producer. Table 2. shows the calculated (Spindle Headstock Version 2.8) values [23] of the optimized design. Figure 34 shows the comparison between the original and optimized designs.

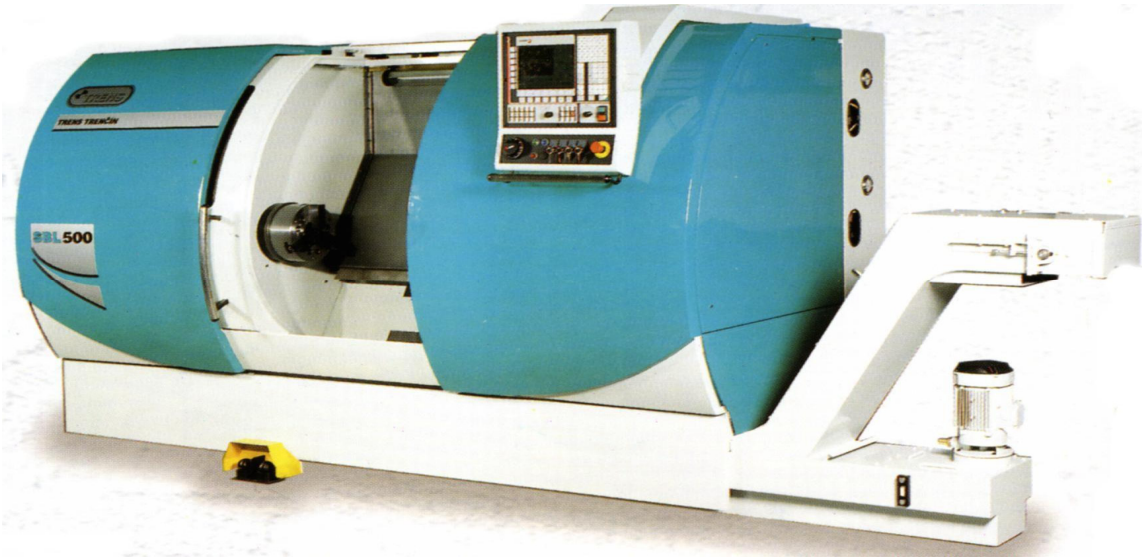


**Figure 31.** CNC Lathe SBL 500

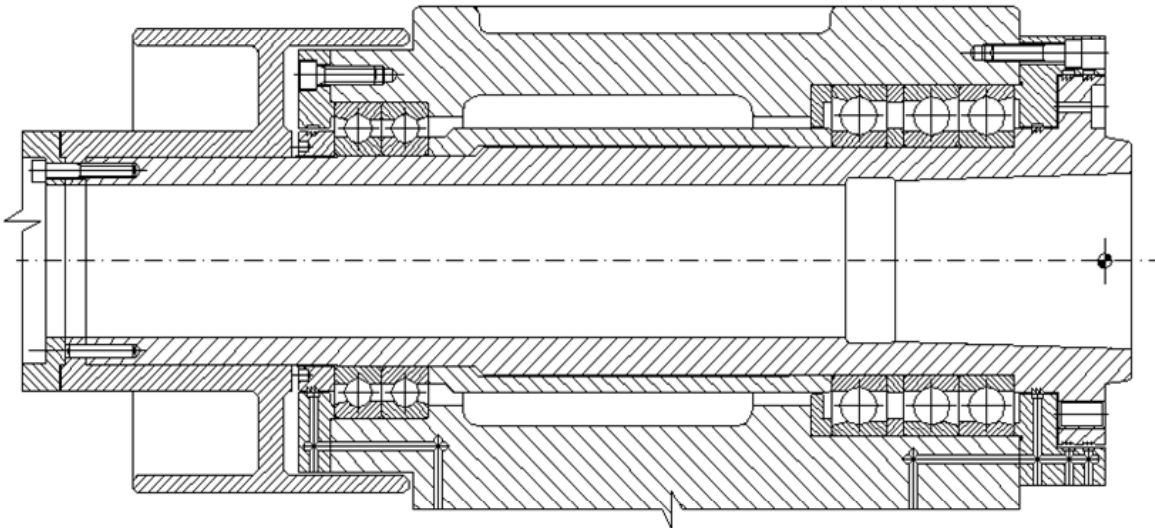


**Figure 32.** Original design of SBL 500

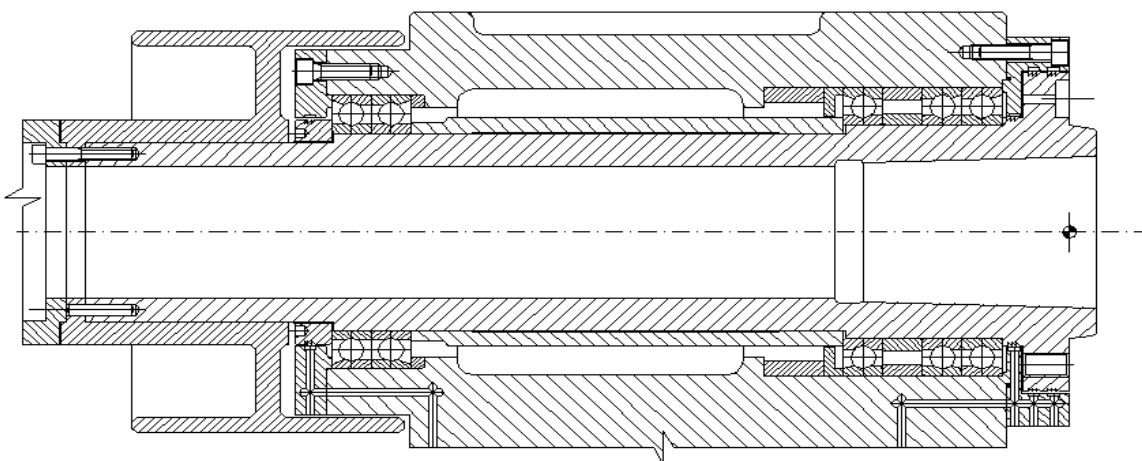


**Figure 33.** Optimized design of SBL 500

		Unit	Value	Notice [%]
Total axial stiffness	$C_a$	[N/ $\mu\text{m}$ ]	372	
Total radial stiffness	$C_r$	[N/ $\mu\text{m}$ ]	351	
Total spindle displacement $y_r$		[ $\mu\text{m}$ ]	18,45	
displacement forces resulting from		[ $\mu\text{m}$ ]		
- the bending moments $y_{Mo}$		[ $\mu\text{m}$ ]	9,79	53,0
- the bearing compliance $y_L$		[ $\mu\text{m}$ ]	6,16	33,5
- the skidding $y_t$			2,49	13,5
Limited frequency of rotation $n_c$		[ $\text{min}^{-1}$ ]	2695	unfit
Life-time $T_h$		[hour ]	5175	unfit
Distance between supports $L$		[mm]	327	

**Table 2.** Calculated values of optimized design

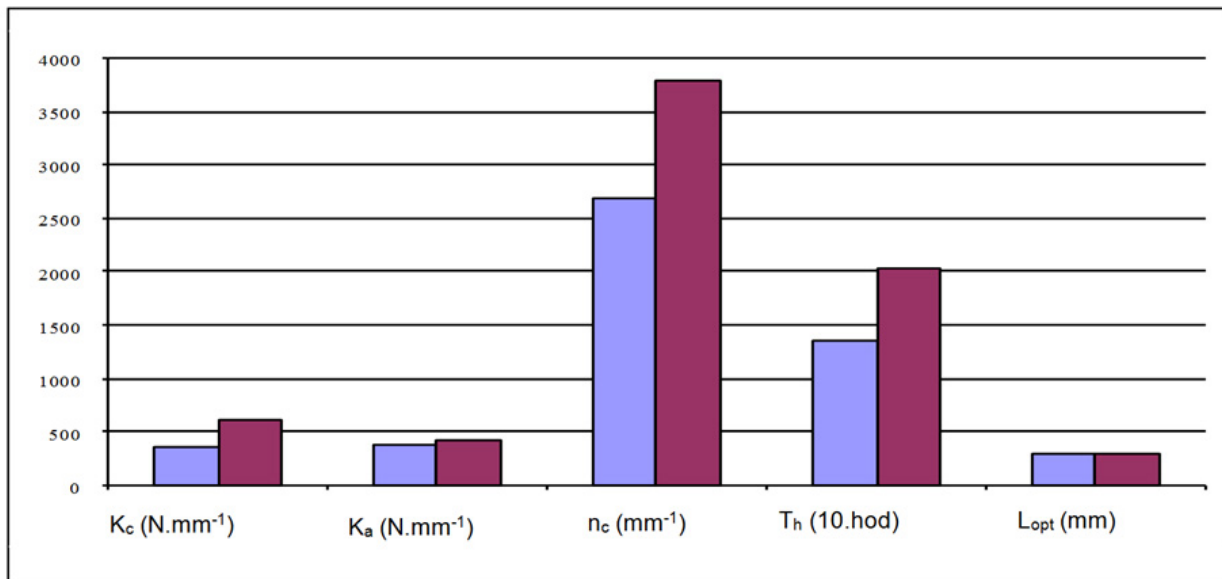


**Figure 34.** Headstock of SBL 500,  Original design,  Optimized design

## 6.2. Dynamic analysis

The most valuable advantage of this system is the possibility of calculating dynamic stiffness at different revolving frequencies of the spindle. The given mathematical model was verified on a number of spindles with programs which enabled the calculation of natural frequencies (COSMOS). The results were in good compliance [24].

The verified spindle, which complied with research findings, was reduced to a three discrete parts. The dynamic mathematical model described above was used to calculate the natural frequencies and dynamic deflections. Table 3 compares calculated and experimental values.

Frequency	Calculated	Experimental	Difference
$f_1$ (Hz)	1 201	940	+27,8 %
$f_2$ (Hz)	1 727	1610	+7,3 %
$f_3$ (Hz)	10 605	-	-

**Table 3.** Experimental and calculated values of frequencies

The results can be considered as correct, in spite of the relatively large difference in values (28 %) in the first frequency. This is as a result of the fact that the dimensions of the additional rotating parts are not included. If these parts were included in the calculation, the values of the calculated natural frequencies would be smaller.

An example of the graphic output of calculated values is shown in Figure 35, [23]. The chart shows the dynamic deflection of the spindle reduced to three masses. The first two resonant frequencies of the optimized spindle are marked on the chart.

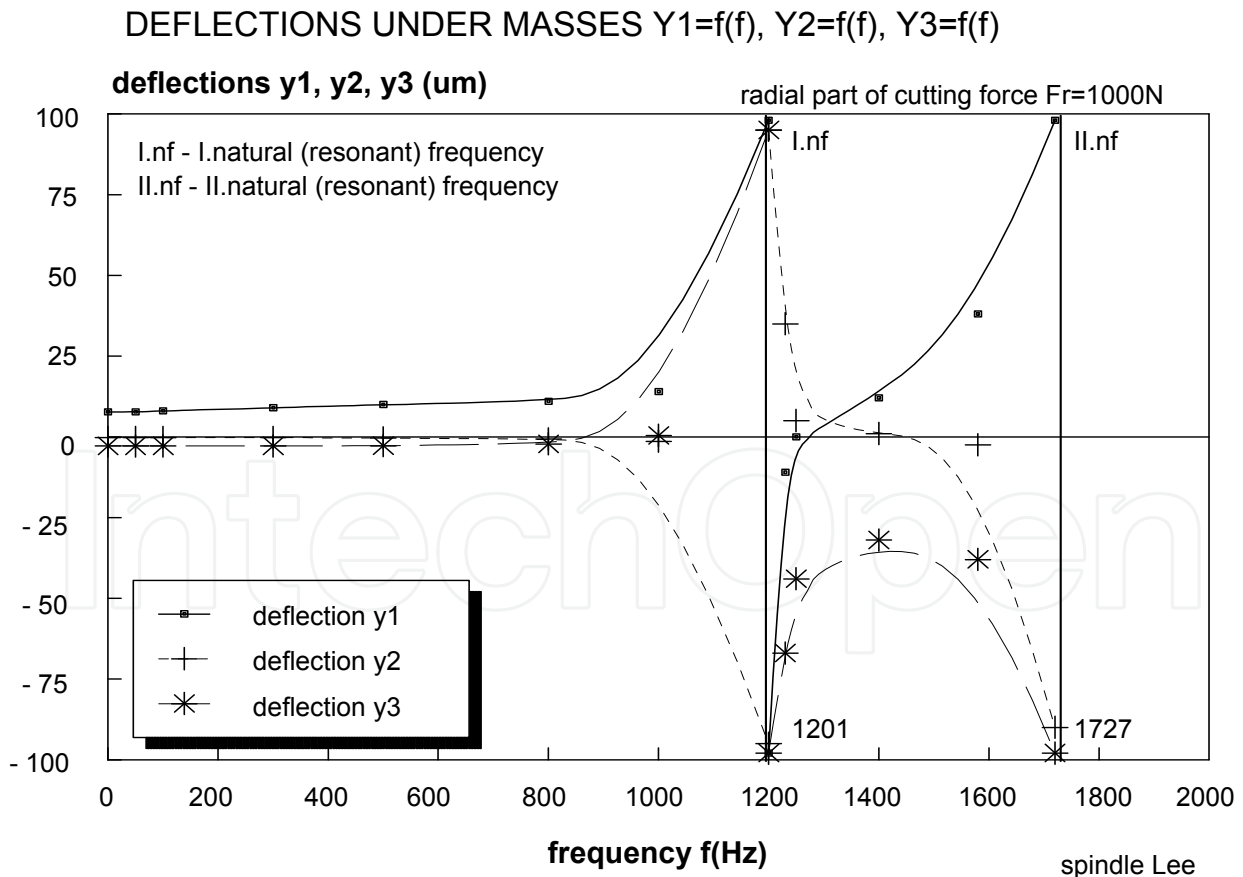


**Figure 35.** Dynamic deflections of the spindle according to research findings [7]

### 6.3. Conclusion

One of the main requirements in designing new spindle housing systems is the ability of the design to be quickly applied to real world practice. The methodologies of calculation that were created must be verified, and models must be adapted into a suitable user friendly, computerized format. The models must illustrate the real characteristics of a spindle housing system.

In this design process, only one variable or parameter was changed and the optimal configuration was identified. The results calculated for a static analysis of the SBL Headstock are presented in Table 2 and Figure 33. The dynamic analysis results are presented in Table 3 and Figure 35. The calculated results were verified with experimental measurements. The difference between measured and calculated values is relatively small.

There is no doubt that the re-design has been a success story, and has proven to be highly effective in the identification of optimal SBS design. More detailed information can be read in [22], [23] and its application can be seen in the machine tools made by TRENS Inc., The SBL Lathe was presented in the Mechanical Engineering Exhibition in Nitra in 2010 and in the EMO Exhibition in Düsseldorf in 2011.

## 7. Nomenclature

N - high-speed ability  
 $\delta$  – elastic compression  
 F – external load  
 P - roller loading  
 E - modulus of elasticity of the material  
 J – quadratic moments of inertia  
 i – number of bearings  
 $\alpha$  – contact angle  
 D, d – diameter  
 n – high spindle revolutions  
 l – distance of curvature centre  
 K - stiffness  
 $\gamma$  – pitch angle  
 O – centre

## INDEXES

a – axial direction  
 r radial direction  
 z – built-in state  
 l – referring to its bearing  
 0 – roller loaded to the maximum

j – circumference roller  
A – external ring  
I – internal ring  
m – medium value  
w - roller bearing

## Author details

Lubomír Šooš

*STU Bratislava, Institute of manufacturing systems, environmental technology and quality management, Bratislava, Slovakia*

## 8. References

- [1] Weck, M., - Hennes, N. - Krell, M. (1999): Spindel and Toolsystems with High Damping. In: *Cirp Annals-manufacturing Technology - CIRP ANN-MANUF. TECHNOL* , vol. 48, no. 1, pp. 297-302, 1999..
- [2] Marek, J a kol.: *Konstrukce CNC obráběcích strojů*. MM Publisching, s.r.o., Praha 2010, ISBN 978-80\_254-7980-3, 419 s p.
- [3] Lee, D. - Sin, H. - Sun, N. (1985) Manufacturing of a Graphite Epoxy Composite Spindle for a Machine Tool. *CIRP*, 34, number 1, pp. 365 -369.
- [4] Šooš, L. (2008) Spindle headstock - the heart of machine tool. In: *Machine Design: On the occasion of 48th anniversary of the Faculty of Technical Sciences: 1960-2008*, Novi Sad: University of Novi Sad. ISBN 978-86-7892-105-6., pp. 335-340.
- [5] Šooš, L. (2008) Quality of design engineering: Case of machine tools headstock. In: *Quality Festival 2008 : 2nd International quality conference*. - Kragujevac, May 13-15, 2008. Kragujevac: University in Kragujevac, ISBN 978-86-86663-25-2.
- [6] Šooš, L. (2008) Contribution to the research of static and dynamic properties of CNC turning machine In: *Strojnícky časopis = Journal of Mechanical engineering*. ISSN 0039-2472. - Roč. 59, č. 5-6 (2008), pp. 231-239
- [7] Javorčík, L. - Šooš, L. - Zon, J. (1991) Applied software technology for designing a bearing housing fitted with rolling bearing arrangemant. in: "ICED 91". Zurich, August, 1991. pp.1228-1233.
- [8] Šooš, L. – Javorčík, L.- Šarkan, P. (1995) An inteligent drive unit for Machine Tools. In.: *The first world congress on Intelligent manufacturing porceedings, university of Puerto Rico*, 13-17. February 1995, pp. 344-352.
- [9] Demeč, P. (2001) *Presnosť obrábacích strojov a jej matematické modelovanie*. - 1. vyd. - Košice: Technická univerzita v Košiciach. - 146 p. - ISBN 80-7099-620-X, (in Slovak).
- [10] Šooš, L. (2008) Criteria for selection of bearings arrangements. In: *32. Savetovanje proizvodnog mašinstva Srbije sa međunarodnim učesćem = 32nd Conference on production engineering of Serbia with foreign participants: Zbornik radova =*

- Proceedings. - Novi Sad, 18.-20. 9. 2008. - Serbia: Fakultet tehničkih nauka. - ISBN 978-86-7892-131-5. - 395-399 p.
- [11] Šooš, L. (2010) New methodology calculations of radial stiffness nodal points spindle machine tool. In: International symposium on Advanced Engineering & Applied Management - 40th Anniversary in Higher Education: Romania /Hunedoara/ 4-5 November, 2010. - Hunedoara: Faculty of Engineering Hunedoara. - ISBN 978-973-0-09340-7. - III-99 - III-104.
- [12] Šooš, L. (2011) Approximate methodology calculations of stiffness nodal points. In: World Academy of Science, Engineering and Technology. - ISSN 2010-376X. - Year 7, Issue 80, pp. 1390-1395.
- [13] Harris, T.A.: (1966) Rolling Bearing Analysis. New York - London - Sydney, 1966, 481 ps.
- [14] Balmont, V.B. - Russkich, S.P.: (1978) Rasčet radialnoj žestkosti radialno - upornogo podšipnika. Trudy instituta. M., Specinformcentr VNIPPa, 69, 1978, č.1, s..pp. 93 - 107.
- [15] Kovalev, M.P.- Narodeckij, M.Z.: (1980) Rasčet vysokotočnych šarikopodšipnikov. 2 vyd. Moskva, Mašinstroenie 1980. 279s p.
- [16] Šooš, L. (2008) Radial stiffness of nodal points of a spindle. In: MATAR Praha 2008. Part 2: Testing, technology: Proceedings of international congresss. - Prague 16th-17th September, Brno 18th September 2008. - Praha: České vysoké učení technické v Praze - ISBN 978-80-904077-0-1. - pp. 43-47.
- [17] Šooš ŠOOŠ, L.- BÁBICSábics, J.: (1989) Axiálna tuhosť vysokootáčkových vretien obrábacích strojov. In.: Strojírěnství, 39, 1989, č.2, pp s. 86-91.
- [18] Šooš, L. - Šarkan, P. (2004) Design of spindle –bearing arrangement of angular ball bearings. In.: MMA 94: Fleksibilne tehnologije: 11th International conference on Flexible Technologies. Novi Sad, 8 – 9.6.2004. - Novi Sad: Institut za proizvodno mašinstvo -pp. 271-275.
- [19] Šooš, L.- Valčuha, Š. - Bábics, J.: PV 08651-88 Zariadenie na skúšanie valivých ložísk [Patent].
- [20] Šooš, L.: Generátor skladaných rotačných pohybov. - 2009. - Číslo úžitkového vzoru: SK 5363. - Dátum nadobudnutia: 22. 12. 2009, [Patent].
- [21] Šooš ŠOOŠ, L.: Duplo pohon, realita alebo vízia? In: Acta Mechanica Slovaca. - ISSN 1335-2393. - Roč. 10, č. 2-A / konf.(heslo) Celoštátna konferencia s medzinárodnou účasťou. 8. ROBTEP 2006. Jasná - Nízke Tatry, 31.5.-2.6.2006 (2006). - Košice : Technická univerzita v Košiciach, spp. 515-518
- [22] Šooš, L. Contribution to the research of static and dynamic properties of CNC turning machine. In: Strojnícky časopis = Journal of Mechanical engineering. - ISSN 0039-2472. - Roč. 59, č. 5-6 (2008), pp. 231-239.
- [23] Šooš, L.: Spindle - housing system SBL 500 CNC. In: Eksploatacja i Niezawodność = Maintenance and reliability. - ISSN 1507-2711. - Č. 2 (2008), pp. 53-56.

- [24] Šooš, E. New methodology calculations of radial stiffness nodal points spindle machine tool. In: International symposium on Advanced Engineering & Applied Management - 40th Anniversary in Higher Education: Romania /Hunedoara/ 4-5 November, 2010. - Hunedoara: Faculty of Engineering Hunedoara, 2010. - ISBN 978-973-0-09340-7. - III-99 - III-104.

IntechOpen

IntechOpen